

AD-A079 955

AERO NAUTICAL RESEARCH LABS MELBOURNE (AUSTRALIA)

F/G 13/10

THE INFLUENCE OF WAKE PATTERN ON THE RUDDER FORCE OF A SHIP MOD--ETC(U)

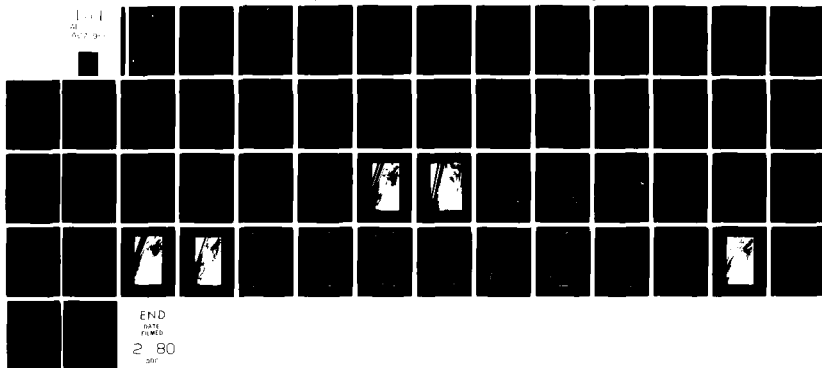
APR 79 N WATHESON

UNCLASSIFIED

ARL/AERO NOTE-389

NL

1 of 1
24
A079 955



✓
LEVEL

(12)
B.S.



AD A 079955

DEPARTMENT OF DEFENCE
DEFENCE SCIENCE AND TECHNOLOGY ORGANISATION
✓**AERONAUTICAL RESEARCH LABORATORIES**

MELBOURNE, VICTORIA

AERODYNAMICS NOTE 389

**THE INFLUENCE OF WAKE PATTERN
ON THE RUDDER FORCE OF A SHIP MODEL
IN A DEEP SEA**

by
N. MATHESON

DDC FILE COPY

Approved for Public Release



DDC
RECEIVED
JAN 29 1980
A

© COMMONWEALTH OF AUSTRALIA 1979

COPY No 22

APRIL 1979

80 1 28 005

THE UNITED STATES NATIONAL
TECHNICAL INFORMATION SERVICE
IS AUTHORIZED TO
REPRODUCE AND SELL THIS REPORT

APPROVED
FOR PUBLIC RELEASE



DEPARTMENT OF DEFENCE

Campbell Park Offices
CANBERRA, A.C.T. 2600

IN REPLY QUOTE: OMS 262/6/22

17 January 1980

Mr Paul Klinefelter
Deputy Director
Directorate of Technical Services
Defense Documentation Center
Cameron Station
Alexandria Virginia 22314
USA

Through Defence Attache US Embassy, Canberra

For Information : Counsellor Defence Science
(without attachment)

AUSTRALIAN DOCUMENTS FOR DDC

12 Copies	MRL-R-725	AR-001-369
" "	ARL-AERO-NOTE-389	AR-001-721
" "	MRL-R-752	AR-001-832
" "	MRL-R-756	AR-001-833
" "	ERL-0099-TR	AR-001-893
" "	ERL-0104-TR	AR-001-905

ALL FOR PUBLIC RELEASE

V. Elder
(V. ELDER)
Officer-in-Charge
Document Exchange Centre

Defence Information Services Branch

11 Apr 79

12 55

AR-001-721

DEPARTMENT OF DEFENCE
DEFENCE SCIENCE AND TECHNOLOGY ORGANISATION
AERONAUTICAL RESEARCH LABORATORIES

14 ARL/AERO NOTE-389

AERODYNAMICS NOTE 389

6 THE INFLUENCE OF WAKE PATTERN
ON THE RUDDER FORCE OF A SHIP MODEL
IN A DEEP SEA

by
10 N./MATHESON

SUMMARY

The results of wind tunnel tests are given which were aimed at overcoming a steering problem on a 33 000 tonne bulk carrier. The ship, as originally built, suffered from vibration and cavitation problems caused by the propeller working in non-uniform flow. A propeller tunnel had been fitted which satisfactorily overcame these problems, but it made the ship much less manoeuvrable, especially at low speed in shallow water.

It was considered that vortex generators could offer an alternative to the propeller tunnel for improving the flow into the propeller without introducing any adverse effects on the steering. Several vortex generator sets were evolved which increased the sideforce produced by the rudder, by up to 44%, but none of them produced an equal or more uniform velocity distribution of the flow into the propeller compared with the tunnel. Since the most important requirement was to eliminate vibration and cavitation, it was concluded that the propeller tunnel could not be replaced by vortex generators.

Accession For

NTIS G.A.R.I.

DOC TAB

Unpublished

Classification

POSTAL ADDRESS: Chief Superintendent, Aeronautical Research Laboratories,
Box 4331, P.O., Melbourne, Victoria, 3001, Australia.

Classification Codes

Dist. Available/or
special

008 650 LMA

DOCUMENT CONTROL DATA SHEET

Security classification of this page: Unclassified

1. Document Numbers (a) AR Number: AR-001-721 (b) Document Series and Number: Aerodynamics Note 389 (c) Report Number: ARL-Aero-Note-389		2. Security Classification (a) Complete document: Unclassified (b) Title in isolation: Unclassified (c) Summary in isolation: Unclassified										
3. Title: The Influence of Wake Pattern on the Rudder Force of a Ship Model in a Deep Sea												
4. Personal Author(s): Matheson, N.		5. Document Date: April, 1979										
		6. Type of Report and Period Covered:										
7. Corporate Author(s): Aeronautical Research Laboratories		8. Reference Numbers (a) Task: AUS 76/225 (b) Sponsoring Agency:										
9. Cost Code: 557700												
10. Imprint Aeronautical Research Laboratories, Melbourne		11. Computer Program(s) (Title(s) and language(s)):										
12. Release Limitations: Approved for public release												
<table border="1"> <tr> <td>12-0. Overseas:</td> <td>N.O.</td> <td>P.R.</td> <td>1</td> <td>A</td> <td>B</td> <td>C</td> <td>D</td> <td>E</td> </tr> </table>				12-0. Overseas:	N.O.	P.R.	1	A	B	C	D	E
12-0. Overseas:	N.O.	P.R.	1	A	B	C	D	E				
13. Announcement Limitations: No limitation												
14. Descriptors: Cargo ships Marine propellers Ship maneuvering Ship models Marine rudders		15. Cosati Codes: Ship Vibration 1310 Wind tunnel models 2011 Cavitation 1402 Wakes Vortex Generators										

16. ↘

ABSTRACT

The results of wind tunnel tests are given which were aimed at overcoming a steering problem on a 33 000 tonne bulk carrier. The ship, as originally built, suffered from vibration and cavitation problems caused by the propeller working in non-uniform flow. A propeller tunnel had been fitted which satisfactorily overcame these problems, but it made the ship much less manoeuvrable, especially at low speed in shallow water.

It was considered that vortex generators could offer an alternative to the propeller tunnel for improving the flow into the propeller without introducing any adverse effects on the steering. Several vortex generator sets were evolved which increased the sideforce produced by the rudder, by up to 44%, but none of them produced an equal or more uniform velocity distribution of the flow into the propeller compared with the tunnel. Since the most important requirement was to eliminate vibration and cavitation, it was concluded that the propeller tunnel could not be replaced by vortex generators.



CONTENTS

	Page No.
NOTATION	
1. INTRODUCTION	1
2. EXPERIMENTS AND EQUIPMENT	1
2.1 Experimental Procedure	1
2.2 Experimental Equipment	2
2.2.1 Model	2
2.2.2 Vortex Generators	2
2.2.3 General Equipment	3
3. EXPERIMENTAL RESULTS	3
3.1 Bare Hull, and Model fitted with the Propeller Tunnel	3
3.1.1 Axial Velocity Distributions in the Propeller Plane	3
3.1.2 Surface Flow Patterns	3
3.1.3 Side Force	4
3.1.4 Resistance	4
3.2 Model Fitted with Vortex Generators	4
3.2.1 Vortex Generator Set No. 1	5
3.2.2 Vortex Generator Set No. 2	5
3.2.3 Vortex Generator Set No. 3	6
3.2.4 Vortex Generator Set No. 4	6
3.2.5 Vortex Generator Set No. 5	6
3.2.6 Vortex Generator Set No. 6	7
3.2.7 Other Vortex Generator Arrangements	7
3.2.8 Resistance of the Model fitted with Vortex Generators	7
4. CONCLUDING REMARKS	7
REFERENCES	9
APPENDICES	10
FIGURES	18
DISTRIBUTION	

NOTATION

C_D	=	$D/(\frac{1}{2}\rho U^2 S)$	= Resistance coefficient
C_Y	=	$Y/(\frac{1}{2}\rho U^2 S)$	= Side force coefficient
D	=		Resistance
h	=		Height of vortex generator
L	=		Length of model (or ship)
l	=		Length of vortex generator
l_f	=		Position of the forward tip of the vortex generator; distance measured along the keel centreline from station no. 2 to the tip of the vortex generator, positive in the aft direction
R	=		Radius of propeller
R_N	=	UL/ν	= Reynolds number
r	=		Radius from centre of propeller shaft in the propeller plane, at which wake velocities were measured
S	=		Surface area of model (or ship)
U	=		Freestream velocity
u	=		Axial velocity of the flow in the propeller plane
Y	=		Side force
y_a	=		Distance around girth of hull from keel centreline to aft tip of vortex generator
y_f	=		Distance around girth of hull from keel centreline to forward tip of vortex generator
α	=		Angle of incidence of rudder measured from the centreline plane of the model, positive for trailing edge of rudder to starboard
β	=		Angle of incidence of vortex generator to surface streamline
θ	=		Angular position in the propeller plane at which axial velocities were measured (origin at top dead centre and measured as positive in a clockwise direction when viewed from aft)
ν	=		Kinematic viscosity
ρ	=		Density

1. INTRODUCTION

A 33 000 tonne single screw ship recently launched in Australia, suffered from vibration and propeller cavitation problems which were caused by the propeller working in an uneven velocity distribution. These problems had been cured by fitting a propeller tunnel to the stern to create a more uniform velocity distribution. However, the propeller tunnel also had the detrimental effect of making the ship less manoeuvrable, especially at low speed in shallow water. This was mainly attributed to the tunnel having an adverse effect on the flow over the top part of the rudder, and to a lesser extent, to an increase in directional stability caused by the vertical sides of the tunnel which were approximately parallel to the longitudinal axis of the ship.

In this report, the results of a series of wind tunnel tests on a model are given, and this investigation is part of a programme designed to improve the manoeuvrability of the ship. First, the velocity distribution of the flow through the propeller disc and the side force produced by the rudder at incidence were measured for the hull both with and without the propeller tunnel. Second, similar tests were made in an attempt to evolve a set of vortex generators which would give an equal or more uniform velocity distribution of the flow through the propeller disc compared with the propeller tunnel. This would enable the vortex generators to be used instead of the propeller tunnel to cure the vibration and cavitation problems. If this could be done, it was expected that the steering problem would not occur, because the vortex generators would not interfere with the flow over the top of the rudder, nor have a large surface area to increase the directional stability.

2. EXPERIMENTS AND EQUIPMENT

2.1 Experimental Procedure

The tests were made on a reflex (mirror image) model of the below waterline section of the hull mounted in the 2.7m \times 2.1m working section of the low speed tunnel. The model was initially tested with the hull in its original 'as designed' condition, and then with the propeller tunnel fitted. Next, the model was systematically tested with different size vortex generators at various angles of incidence attached to the stern at a number of positions. In this way it was expected that a suitable vortex generator system would be developed which could be used to replace the propeller tunnel. Surface flow visualization, wake survey, resistance, and side force measurements were made to find the effectiveness of each vortex generator system. These tests were made in a similar manner to those in previous investigations with vortex generators attached to the stern of a ship model^{1,2}.

The model tests were initially carried out in the 'deep water' condition. Since the ship operates predominantly in a deep sea it was important to develop a set of vortex generators which gave satisfactory propeller cavitation and hull vibration characteristics under this condition. Provided a satisfactory generator system had been developed for the deep sea case, tests were then to be made in simulated 'shallow water', where the steering problem is more acute.

Using a reflex model and testing it in a wind tunnel prevents free surface (Froude number) effects from being represented. However, in the present case wavemaking was not expected to influence the results to any great extent because the vortex generators were all placed well below the waterline near the keel. Previous wind tunnel and towing tank tests of a ship model fitted with vortex generators have shown little difference between corresponding axial velocity distributions of the flow into the propeller¹.

Unless stated otherwise, the tests were made at a Reynolds number of 10^7 , based on model length between perpendiculars. Since the ship operates at a Reynolds number of about 1.1×10^9 scale effects may be significant. However, the model results should be conservative since the boundary layer is relatively thicker on the model than the ship. Physical limitations of the wind tunnel prevented any further reduction in scale effect by testing at higher Reynolds numbers.

Additional effects not simulated are propeller action, structural roughness, and fouling of the hull surface. While the propeller has a favourable influence on the flow over the stern, hull roughness and fouling are detrimental. However, some allowance can be made for these effects when applying the model results to the full scale ship^{1,2}.

2.2 Experimental Equipment

2.2.1 Model

All tests were made with a 1/59.33 scale reflex model which was approximately 2.9m long. The main dimensions of the ship from which the model was scaled are given in Table 1, and the section lines and stern arrangement are shown in Figures 1 and 2 respectively. The propeller tunnel for the ship is shown in Figure 3. The model was fitted with bilge keels. Studs were also attached to the bow to produce turbulent flow over the surface of the model similar to that which occurs naturally over the surface of the full size ship. Provision was made for testing the model in either the full load or ballast condition.

TABLE 1 - Main ship particulars

1. Length between perpendiculars	163.6m
2. Length - sections 0 to 10	162.8m
3. Breadth	25.0m
4. Draught	9.81m
5. Displacement	33 000t
6. Wetted surface coefficient	6.130
7. Block coefficient	0.802
8. Full load service speed	16 kn
9. Closed aperture stern	
10. Semi balanced rudder, 3.96m chord, 6.48m span	
11. Four blade controllable pitch propeller, 6.00m diameter	

2.2.2 Vortex Generators

Vortex generators redirect relatively high momentum fluid along helical paths to mix with retarded fluid near the surface of the ship or model. The increase in energy of the fluid counters, to some extent, any tendency for separation to occur over the stern, as well as modifying the velocity distribution of the flow through the propeller disc and over the rudder. For good performance the vortex generators should be highly effective over a wide range of conditions and only incur a small power penalty. These requirements are mutually conflicting, and a number of tests are usually needed to refine the design to produce a satisfactory velocity distribution within an allowable power limit.

Although there are a number of different types of vortex generators, only vane type generators with a triangular planform were selected for the tests since they are known to perform very well under a wide variety of conditions^{3,4}, including those likely to be experienced on the stern of a ship. Each generator had a thin symmetrical bi-convex section and was tapered in the spanwise direction away from the hull surface. The generators were fitted to the hull with their span wise axis at about 2/3 of their length from the forward tip normal to the hull surface.

2.2.3 General Equipment

Local velocities in the plane of the propeller were measured using a rake of pitot probes. The probes were mounted on an arm which was rotated about the centre of the propeller shaft so that the velocity of the flow could be determined at selected angular positions and at various radii.

Both the resistance of the model and the side force produced by the rudder were measured using an external mechanical drag balance. All results were corrected for the effects of blockage, and a small longitudinal pressure gradient existing in the working section of the wind tunnel.

The flow pattern on the surface of the model was made visible using kerosene mixed with a little french chalk. This method gave good results although gravity has influenced the patterns, especially in the comparatively low surface shear region at the stern. The surface flow patterns must therefore be interpreted bearing in mind that gravity effects are present.

3. EXPERIMENTAL RESULTS

The basic purpose of the tests was to develop a set of vortex generators that produce a velocity distribution of the flow into the propeller which gives satisfactory vibration and cavitation characteristics without impairing manoeuvrability.

In the following sections the results for six of the more promising vortex generator configurations are compared with the results for the bare hull and the model fitted with the propeller tunnel.

3.1 Bare Hull, and Model fitted with the Propeller Tunnel

3.1.1 Axial Velocity Distributions in the Propeller Plane

The axial velocity distribution of the flow in the plane of the propeller of the model, with and without the propeller tunnel, at radius ratios of 1.23, 0.96, 0.68 and 0.41, are shown in Figure 4. The experimental results are tabulated in Appendix 1.

As expected, in the case of the bare hull relatively low axial velocities occurred over the top of the propeller disc at radius ratios of 1.23 and 0.96 for ϑ from $\pm(0^\circ$ to $30^\circ)$, compared with the velocities for ϑ from $\pm(70^\circ$ to $160^\circ)$. Further in towards the centre of the propeller disc at radius ratios of 0.68 and 0.41 the axial velocities for ϑ from $\pm(70^\circ$ to $160^\circ)$ were much lower, and the velocity distributions for ϑ from $\pm(0^\circ$ to $160^\circ)$ were more uniform than in the outer sections of the disc at $r/R=0.96$ and 1.23. Over the lower section of the propeller disc for ϑ from $\pm(160^\circ$ to $180^\circ)$ the axial velocity ratios were quite small from the hub to the tip of the disc due to the closed propeller aperture.

The velocity distribution formed with the propeller tunnel and with the bare hull were similar in shape. A significant increase in velocity had been expected for ϑ from $\pm(0^\circ$ to $10^\circ)$, but in fact there was no improvement in this region except for a small increment at $r/R=0.96$. However, the tunnel increased the velocity for ϑ from $\pm(10^\circ$ to $80^\circ)$ at radius ratios of 1.23, 0.96 and 0.68. There was a significant improvement in the uniformity of the velocity distribution at $r/R=0.68$, but only small improvements at radius ratios of 1.23 and 0.96. The distribution at $r/R=0.41$ was less uniform with the propeller tunnel than for the bare hull. Overall, the propeller tunnel produced a more even velocity distribution of the flow through the propeller disc, but the improvement was less than had been anticipated.

3.1.2 Surface Flow Patterns

The surface flow patterns over the stern of the bare hull, and the model with the propeller tunnel, are shown in Figure 5. There was little difference between the patterns. In each case there was a small region of separated flow just above and below the propeller shaft which resulted in low axial velocities of the flow through the propeller plane for ϑ between approximately $\pm(0^\circ$ to $20^\circ)$ and $\pm(160^\circ$ to $180^\circ)$.

3.1.3 Side Force

The side force coefficients produced by placing the rudder at a number of angles of incidence are shown in Figure 6, and tabulated in Appendix 2. The points plotted in Figure 6 are the means of the coefficients found for the rudder at the same angle of incidence to port and starboard. The results show that the propeller tunnel produces a 7% increase in the side force coefficient at all angles of incidence. This shows that the masking of the top of the rudder by the propeller tunnel is more than balanced by the increase in velocity of the fluid in which the remainder of the rudder is working. Furthermore, the results indicate that the reduction in steering performance is due to an increase in directional stability caused by the propeller tunnel.

3.1.4 Resistance

The resistance coefficients for the model both with and without the propeller tunnel are plotted in Figure 7 and tabulated in Appendix 3. The resistance coefficients for the bare hull followed the normal trend for this type of hull. At a Reynolds number of 10^7 , the resistance coefficient for the model fitted with the propeller tunnel was 0.00020 (approximately 5%) greater than the resistance coefficient for the bare hull.

3.2 Model Fitted with Vortex Generators

The propeller tunnel was removed from the model and a series of tests made with vortex generators attached to the stern. The position, angle of attack, height, and number of vortex generators were varied systematically. All the generators had an aspect ratio of 1.1 which was found to be satisfactory in previous tests with ship models^{1,2}. In addition, they were arranged to produce co-rotating vortices symmetrical about the keel centreline since this had also been shown to be very effective. The position and size of each vortex generator was restricted so that it did not extend beyond the maximum draft and beam of the hull in order to minimise the risk of accidental damage during service. The generators were also located so that they did not cause any fouling of the engine water inlets or outlets.

Using the experience gained from similar investigations^{1,2}, coupled with some initial tests, the basic requirements for size, incidence, and positioning of the generators soon became apparent. The most effective position was found to lie near the turn of the bilge between the 0.61m and 2.44m waterline, and between station 1 and 2¼. The generators could not be placed closer to the keel centreline because they would extend below the bottom of the hull. When placed further away from the keel centreline they were less effective because the local turbulent boundary layer was much thicker. It was found preferable to use reasonably small generators at an incidence of about 20° rather than larger generators at lower incidence. Prohibitively high power penalties occurred if the generators were too large or if they were set at appreciably higher angles of attack. In addition, it was found that the best results were obtained with four vortex generators, two port and two starboard. More generators were less effective because they had to be very small to keep the power penalty within a reasonable limit. Similarly, two generators, one port and one starboard, did not produce a sufficiently uniform velocity distribution.

The results for six of the more promising sets of vortex generators are presented in this report. The relative position of each of the six sets is shown to scale in Figure 8, while the size and location of each generator is given in Table 2. Similar vortex generators were fitted to the port and starboard sides of the hull. The axial velocity ratio distributions for the flow in the plane of the propeller are tabulated in Appendix 4, and the side force coefficients produced by placing the rudder at various angles of incidence are tabulated in Appendix 5. The resistance coefficients for the model fitted with each vortex generator system are given in Appendix 6.

TABLE 2 - Vortex generator size and location. (Similar generators fitted to port and starboard sides of the hull.)

Generator set no.	h (mm)	l (mm)	y_f (mm)	y_a (mm)	l_f (mm)	β (°)
1	$h_1=12.7$	$l_1=46$	128.5	147.3	-84	20
	$h_2=6.4$	$l_2=23$	43.7	55.9	264	20
2	$h_1=10.7$	$l_1=38$	137.2	152.9	-74	20
	$h_2=8.4$	$l_2=30$	72.4	87.9	173	20
3	$h_1=10.7$	$l_1=38$	160.0	176.5	-64	20
	$h_2=8.4$	$l_2=30$	115.8	130.0	127	20
4	$h_1=10.7$	$l_1=38$	160.0	176.5	-64	20
	$h_2=8.4$	$l_2=30$	125.7	138.4	81	20
5	$h_1=10.7$	$l_1=38$	150.4	166.4	-64	20
	$h_2=8.4$	$l_2=30$	125.7	138.4	81	20
6	$h_1=10.7$	$l_1=38$	150.4	166.4	-64	20
	$h_2=8.4$	$l_2=30$	137.2	150.1	13	20

3.2.1 Vortex Generator Set No. 1

The axial velocity distribution of the flow in the plane of the propeller is shown in Figure 9. The generators were positioned with the aim of increasing the velocity of the flow in both the upper and lower segments of the propeller disc near $\vartheta=0^\circ$ and 180° respectively. However, compared with the results for the propeller tunnel (also plotted in Figure 9) the velocity distribution with the vortex generators was not satisfactory. In particular, there was a large reduction in velocity in the region $\vartheta=\pm(0^\circ \text{ to } 120^\circ)$ at $r/R=0.96$, and $\vartheta=\pm(0^\circ \text{ to } 40^\circ)$ at $r/R=0.68$ and 0.41 , and there was a significant increase in velocity in the region $\vartheta=\pm(50^\circ \text{ to } 180^\circ)$ for $r/R=0.68$ and 0.41 , resulting in an overall velocity distribution which was far less uniform than that obtained with the propeller tunnel.

The surface flow pattern over the stern of the model is shown in Figure 10. Between the keel and the propeller shaft the pattern appears to be slightly better than that formed with the propeller tunnel, but above the propeller shaft it is worse.

The side force coefficients for the model are shown in Figure 6. Compared with the bare hull, there was an increase in the side force coefficient of 18% at a rudder angle of 15° , and 28% at 25° . There was a nett increase in sideforce because the increase in fluid velocity near the lower section of the rudder ($\vartheta=180^\circ$) had a greater effect on performance than the decrease in velocity near the upper portion of the rudder ($\vartheta=0^\circ$).

3.2.2 Vortex Generator Set No. 2

The aft vortex generators were increased in size and moved further forward to try to increase the velocity in the region of $\vartheta=180^\circ$, and the forward generators were made slightly smaller but left in about the same position to try to reduce the velocity hump which had occurred for $\vartheta=\pm(70^\circ \text{ to } 150^\circ)$ at $r/R=0.68$ and 0.41 .

The axial velocity distribution of the flow in the propeller plane is plotted with the results for the first set in Figure 9. Again this velocity distribution was not satisfactory because of the very low velocities in the region $\vartheta = \pm(0^\circ \text{ to } 50^\circ)$ at $r/R = 0.96$ and 0.68 , and the high velocity for $\vartheta = \pm(70^\circ \text{ to } 160^\circ)$ at $r/R = 0.96, 0.68$ and 0.41 .

There was a slight improvement in the surface flow pattern formed with this set of generators compared with the first set, as shown in Figure 11.

The side force coefficients shown in Figure 6 were greater for the second set of generators than the first set. This was mainly caused by the relative increase in velocity near the top of the rudder for ϑ between approximately $\pm(20^\circ \text{ to } 100^\circ)$ at $r/R = 0.96$ and 0.68 .

3.2.3 Vortex Generator Set No. 3

These vortex generators were the same size as the previous set, but the aft generators were moved further forward and away from the keel centreline. The forward generators were kept in the same longitudinal position, but were also moved further away from the keel centreline.

The axial velocity distribution of the flow in the propeller plane, shown in Figure 12, was much better than for the previous generators, although it was not considered good enough for them to replace the propeller tunnel. The low velocity region at the top of the propeller disc formed with both of the previous sets of generators had been substantially reduced. However, compared with the velocity distribution for the propeller tunnel, the velocity of the flow was still too high for ϑ between approximately $\pm(50^\circ \text{ to } 170^\circ)$ at $r/R = 0.68$.

The surface flow pattern formed with this set of generators was similar to the pattern formed with the previous generators.

The side force coefficients for the model with these generators are shown in Figure 6. Compared with the bare hull, there was a 48% increase in the side force coefficient at rudder angles of $15^\circ, 20^\circ$ and 25° . These higher side force coefficients were produced by an increase in the velocity of the flow over both the top and bottom sections of the rudder.

3.2.4 Vortex Generator Set No. 4

The forward generators of the fourth set were the same as the forward generators of set no. 3, but the aft generators were again moved further forward and outwards from the keel centreline.

As shown in Figure 12, there was very little difference between the axial velocity distribution for the third and fourth sets of vortex generators, but there was some improvement for ϑ between approximately $\pm(0^\circ \text{ to } 60^\circ)$ at $r/R = 1.23$ and 0.96 .

Because there was very little change in the velocity distribution, the side force coefficients produced by the rudder were only marginally improved from an increase of 48% for set no. 3 to 50% for set no. 4.

3.2.5 Vortex Generator Set No. 5

The forward generators of this set were moved slightly further in towards the keel centreline but were kept at the same longitudinal position. The aft generators were the same as the aft generators of the fourth set.

The axial velocity of the flow in the propeller plane, plotted in Figure 13, showed a small improvement over the outer top dead centre region of the propeller disc compared with the fourth set of generators. However, there was little change in the velocity distribution at $r/R = 0.68$ and relatively high velocities still occurred for ϑ from approximately $\pm(50^\circ \text{ to } 160^\circ)$. Overall, the velocity distribution of the flow into the propeller was still not considered to be sufficiently uniform to recommend replacing the propeller tunnel with vortex generators.

The surface flow pattern formed with the fifth set of generators is shown in Figure 14. While the shape of the pattern is very similar to the shape formed with the bare hull shown in Figure 5, comparison between the two patterns indicates that the very low velocity (separation) regions both above and below the propeller shaft have been reduced in extent. This reflects the improvements found from the wake surveys.

The side force coefficients shown in Figure 6 were slightly improved compared with the fourth set of generators. At a rudder incidence of 15° , 20° and 25° the side force coefficient was 55% greater than obtained with the bare hull.

3.2.6 Vortex Generator Set No. 6

In this case the forward generators were the same as set no. 5, but the aft generators were moved further forward and away from the keel centreline.

The axial velocity distribution of the flow in the propeller plane formed with the sixth set of generators, shown in Figure 13, was significantly worse than the distribution formed with set no. 5. In this case the vortices shed from the fore and aft generators on either side of the hull interacted detrimentally downstream and they were not as effective as the vortices from the fifth set of generators. Consequently, the improvement in side force coefficient compared with the bare hull was reduced to 51% compared with 55% for vortex generator set no. 5.

3.2.7 Other Vortex Generator Arrangements

A number of other generator arrangements were tried in an attempt to produce a more uniform velocity distribution in the propeller plane.

For instance, the aft generator of the first set was moved further downstream in an attempt to further improve the velocity for $\vartheta = \pm(160^\circ \text{ to } 180^\circ)$ at $r/R = (0.41 \text{ to } 1.23)$, and the forward generator was moved further forward and away from the keel centreline in an attempt to improve the velocity at the top of the propeller disc while reducing the velocity in the region $r/R = 0.68$ and $\vartheta = \pm(50^\circ \text{ to } 160^\circ)$. However, the results obtained were no better than those for vortex generator set no. 5. The results of tests with generators of different sizes at various angles of incidence were similar to the results presented earlier. For example, smaller vortex generators reduced the high velocity at $r/R = 0.68$, but failed to improve the flow in the region $\vartheta = 0^\circ$ or 180° .

3.2.8 Resistance of the Model fitted with Vortex Generators

The resistance coefficients for the model fitted with three of the vortex generator sets are plotted in Figure 7, with the results for the bare hull and the model fitted with the propeller tunnel. The resistance coefficients for vortex generator set numbers 3 and 4, and set number 6 are not shown since they are effectively the same as sets 2 and 5 respectively.

The increase in resistance coefficient with the propeller tunnel fitted, and with each vortex generator system, at a Reynolds number of 10^7 is given in Table 3. There was a 5% increase in resistance when the propeller tunnel was fitted, but less than 2% when the generators were fitted. However, because the vortex generators alter the velocity of the flow in the wake more than the propeller tunnel, it was estimated that the increase in power for the ship with vortex generators would be about the same as the increase required with the propeller tunnel.

4. CONCLUDING REMARKS

A propeller tunnel, which had previously been fitted to the stern of a tanker to cure vibration and cavitation problems, made the ship less manoeuvrable especially at low speed in shallow water. The results from wind tunnel tests of a model showed that the propeller tunnel produced a more uniform velocity distribution of the flow into the propeller, but the improvement was less than had been expected. However, it was also found that the side force produced by the rudder at incidence for the model with the

TABLE 3 - Resistance coefficients for the model at $R_N=10^7$.

Model Configuration	C_D	% increase in C_D
Bare hull	0.00383	Base
Propeller tunnel	0.00403	5.2
Vortex generator set no. 1	0.00391	2.1
Vortex generator set no. 2	0.00389	1.6
Vortex generator set no. 3	0.00389	1.6
Vortex generator set no. 4	0.00389	1.6
Vortex generator set no. 5	0.00387	1.0
Vortex generator set no. 6	0.00387	1.0

propeller tunnel was 7% greater than the side force for the bare hull, and the reduction in manoeuvrability was caused by the propeller tunnel increasing the directional stability.

It was considered that fitting vortex generators to the stern might offer a suitable alternative to the propeller tunnel for improving both the velocity of the flow to the propeller and the manoeuvrability of the ship. From wind tunnel tests on a model without the propeller tunnel, a set of vortex generators (set no. 5) was developed which increased the side force produced by the rudder by 55% and made the axial velocity distribution of the flow in the propeller plane more uniform compared with the bare hull. However, no vortex generator system was found which made the velocity distribution of the flow into the propeller significantly more uniform than the velocity distribution produced with the propeller tunnel. In view of this lack of significant improvement in uniformity of the axial velocity distribution of the flow into the propeller, and because the large and costly propeller tunnel already fitted to the ship gives acceptable vibration and cavitation characteristics, it cannot be recommended that vortex generators be used to replace the propeller tunnel, even though they do give a large improvement in rudder sideforce. Some other means for improving manoeuvrability must therefore be found, for example, the stern could be modified to an open aperture, the clearance between the hull and propeller increased, or preferably the rudder could be increased in size.

The model tests originally intended in ballast and 'shallow water' conditions were not made. Since a satisfactory wake velocity distribution could not be obtained for the fully loaded ship in a deep sea there was no point in making these tests.

REFERENCES

1. MATHESON, N. Further studies on a ship model fitted with vortex generators to improve the velocity distribution of the flow into the propeller. Department of Defence, Australian Defence Scientific Service, Aeronautical Research Laboratories, Aerodynamics Note 359, 1975.
2. MATHESON, N. Wind tunnel studies of a ship model using vortex generators to improve wake velocities. Department of Supply, Australian Defence Scientific Service, Aeronautical Research Laboratories, Aerodynamics Note 347, April 1974.
3. CHANG, P.K. Control of flow separation: energy conservation, operational efficiency, and safety. Hemisphere Publishing Corporation, Washington, London, 1976.
4. LACHMAN, C.V. Boundary layer and flow control. Pergamon Press, Oxford, London, 1961.

APPENDIX 1

Axial velocity component ratios of the flow in the propeller plane of the model with and without the propeller tunnel.

θ (°)	u/U							
	$r/R = 1.23$		$r/R = 0.96$		$r/R = 0.68$		$r/R = 0.41$	
	Bare Hull	Prop- eller Tunnel	Bare Hull	Prop- eller Tunnel	Bare Hull	Prop- eller Tunnel	Bare Hull	Prop- eller Tunnel
0	0.27	—	0.33	0.41	0.38	0.36	0.34	0.30
12	0.38	—	0.46	0.50	0.46	0.47	0.38	0.33
24	0.53	—	0.52	0.54	0.46	0.51	0.39	0.39
36	0.61	0.59	0.56	0.57	0.40	0.50	0.38	0.42
48	0.67	0.66	0.61	0.60	0.33	0.43	0.32	0.41
72	0.81	0.82	0.76	0.68	0.39	0.36	0.22	0.30
96	0.91	0.93	0.88	0.86	0.64	0.57	0.25	0.28
120	0.94	0.95	0.92	0.92	0.70	0.62	0.26	0.27
144	0.95	0.95	0.94	0.92	0.64	0.48	0.17	0.10
168	0.94	0.82	0.67	0.47	0.30	0.23	0.10	0.06
180	0.95	0.93	0.23	0.26	0.13	0.22	0.08	0.06
-12	0.43	—	0.43	0.45	0.40	0.44	0.31	0.34
-24	0.56	—	0.49	0.53	0.43	0.52	0.34	0.41
-36	0.63	0.61	0.53	0.57	0.35	0.52	0.34	0.44
-48	0.70	0.68	0.57	0.61	0.26	0.45	0.30	0.43
-72	0.84	0.82	0.67	0.69	0.32	0.36	0.18	0.34
-96	0.93	0.93	0.84	0.86	0.55	0.55	0.18	0.31
-120	0.94	0.95	0.91	0.93	0.65	0.64	0.20	0.32
-144	0.95	0.95	0.92	0.94	0.57	0.56	0.12	0.23
-168	0.95	0.86	0.80	0.70	0.30	0.31	0.06	0.04
-180	0.95	0.94	0.22	0.28	0.13	0.23	0.08	0.05

APPENDIX 2

Side force coefficients for the bare hull, and the model fitted with the propeller tunnel.

Bare Hull		Propeller Tunnel	
$\alpha(^{\circ})$	$C_Y \times 10^4$	$\alpha(^{\circ})$	$C_Y \times 10^4$
0.0	-0.13	0.0	-0.15
4.6	-2.64	4.6	-2.95
7.6	-4.45	7.6	-4.61
12.3	-6.54	12.3	-7.32
17.0	-9.37	17.0	-10.13
21.9	-12.29	21.9	-13.18
28.6	-15.95	28.6	-17.52
-4.6	2.34	-4.6	2.41
-7.6	3.81	-7.6	4.32
-12.3	6.26	-12.3	7.40
-17.0	9.18	-17.0	10.01
-21.9	11.99	-21.9	12.49
-28.6	15.49	-28.6	16.94

APPENDIX 3

Resistance coefficients for the bare hull, and the model fitted with the propeller tunnel.

Bare Hull		Propeller Tunnel	
$R_N \times 10^{-6}$	$C_D \times 10^3$	$R_N \times 10^{-6}$	$C_D \times 10^3$
2.61	4.67	7.57	4.20
3.02	4.71	8.54	4.14
3.38	4.60	9.88	4.06
3.73	4.50	9.42	4.05
4.10	4.42	9.06	4.09
4.75	4.33	8.36	4.13
5.32	4.20	8.04	4.16
6.03	4.11	7.75	4.19
6.70	4.04		
7.29	3.99		
7.85	3.96		
8.52	3.91		
9.17	3.88		
9.75	3.85		
10.01	3.82		
9.46	3.85		
8.83	3.89		
8.20	3.93		
7.56	3.98		
7.00	4.02		
6.37	4.07		
5.71	4.18		
5.06	4.25		
4.45	4.38		
3.95	4.49		
3.58	4.57		
3.20	4.65		
2.78	4.72		
2.38	4.60		

APPENDIX 4

Axial velocity component ratios of the flow in the propeller plane of the model fitted with vortex generator set numbers one to six.

ϑ (°)	u/U							
	Vortex generator Set No. 1				Vortex Generator Set No. 2			
	$r/R=$ 1.23	$r/R=$ 0.96	$r/R=$ 0.68	$r/R=$ 0.41	$r/R=$ 1.23	$r/R=$ 0.96	$r/R=$ 0.68	$r/R=$ 0.41
0	0.34	0.32	0.31	0.22	0.29	0.25	0.21	0.16
12	0.47	0.42	0.32	0.22	0.38	0.40	0.40	0.22
24	0.57	0.40	0.32	0.22	0.52	0.60	0.52	0.26
36	0.62	0.40	0.40	0.25	0.54	0.66	0.62	0.28
48	0.69	0.43	0.57	0.34	0.56	0.72	0.72	0.32
72	0.83	0.62	0.75	0.55	0.82	0.87	0.83	0.43
96	0.91	0.89	0.89	0.68	0.91	0.91	0.89	0.56
120	0.92	0.91	0.90	0.71	0.93	0.92	0.91	0.60
144	0.93	0.92	0.91	0.56	0.94	0.93	0.91	0.47
168	0.94	0.90	0.62	0.28	0.94	0.88	0.58	0.22
180	0.94	0.50	0.26	0.25	0.94	0.33	0.19	0.16
-12	0.46	0.40	0.30	0.21	0.39	0.28	0.26	0.13
-24	0.57	0.38	0.31	0.20	0.54	0.42	0.34	0.15
-36	0.65	0.38	0.41	0.21	0.56	0.62	0.47	0.19
-48	0.71	0.41	0.53	0.25	0.60	0.76	0.58	0.24
-72	0.85	0.62	0.70	0.44	0.86	0.87	0.76	0.28
-96	0.92	0.88	0.86	0.62	0.91	0.90	0.86	0.42
-120	0.93	0.91	0.90	0.70	0.93	0.91	0.88	0.45
-144	0.94	0.92	0.92	0.63	0.94	0.92	0.88	0.37
-168	0.94	0.93	0.68	0.36	0.94	0.90	0.50	0.20
-180	0.94	0.51	0.28	0.26	0.94	0.36	0.19	0.15

APPENDIX 4 (Continued)

ϕ (°)	u/U							
	Vortex generator Set No. 3				Vortex Generator Set No. 4			
	$r/R=$ 1.23	$r/R=$ 0.96	$r/R=$ 0.68	$r/R=$ 0.41	$r/R=$ 1.23	$r/R=$ 0.96	$r/R=$ 0.68	$r/R=$ 0.41
0	0.45	0.45	0.48	0.48	0.53	0.49	0.50	0.46
12	0.45	0.59	0.54	0.44	0.54	0.59	0.53	0.47
24	0.51	0.64	0.57	0.42	0.59	0.66	0.56	0.43
36	0.58	0.69	0.61	0.38	0.67	0.71	0.61	0.38
48	0.68	0.76	0.69	0.34	0.75	0.76	0.67	0.32
72	0.84	0.84	0.80	0.37	0.84	0.84	0.79	0.35
96	0.91	0.90	0.87	0.48	0.91	0.90	0.86	0.46
120	0.92	0.91	0.90	0.51	0.93	0.91	0.90	0.51
144	0.94	0.92	0.90	0.42	0.94	0.92	0.91	0.44
168	0.94	0.91	0.55	0.21	0.93	0.88	0.61	0.20
180	0.95	0.31	0.18	0.15	0.94	0.31	0.18	0.14
-12	0.53	0.53	0.48	0.40	0.59	0.55	0.47	0.43
-24	0.58	0.61	0.46	0.33	0.65	0.61	0.46	0.37
-36	0.66	0.68	0.48	0.29	0.71	0.68	0.48	0.30
-48	0.75	0.74	0.54	0.27	0.79	0.73	0.52	0.24
-72	0.88	0.84	0.73	0.29	0.88	0.83	0.71	0.30
-96	0.93	0.90	0.82	0.40	0.93	0.90	0.81	0.39
-120	0.94	0.91	0.87	0.44	0.93	0.91	0.87	0.43
-144	0.94	0.92	0.86	0.32	0.94	0.92	0.85	0.33
-168	0.94	0.92	0.41	0.17	0.94	0.92	0.48	0.17
-180	0.94	0.33	0.18	0.15	0.94	0.33	0.16	0.13

APPENDIX 4 (Continued)

θ (°)	u/U							
	Vortex generator Set No. 5				Vortex Generator Set No. 6			
	$r/R=$ 1.23	$r/R=$ 0.96	$r/R=$ 0.68	$r/R=$ 0.41	$r/R=$ 1.23	$r/R=$ 0.96	$r/R=$ 0.68	$r/R=$ 0.41
0	0.52	0.47	0.46	0.41	0.41	0.40	0.36	0.37
12	0.57	0.57	0.48	0.42	0.56	0.54	0.42	0.33
24	0.66	0.65	0.50	0.38	0.65	0.62	0.46	0.31
36	0.70	0.70	0.55	0.31	0.70	0.69	0.52	0.28
48	0.76	0.76	0.65	0.29	0.74	0.76	0.58	0.26
72	0.85	0.85	0.78	0.34	0.85	0.84	0.74	0.28
96	0.90	0.90	0.87	0.44	0.91	0.90	0.85	0.36
120	0.93	0.91	0.90	0.48	0.92	0.91	0.90	0.42
144	0.94	0.93	0.90	0.40	0.93	0.92	0.89	0.34
168	0.94	0.88	0.59	0.21	0.93	0.85	0.58	0.20
180	0.95	0.31	0.16	0.14	0.94	0.30	0.16	0.14
-12	0.61	0.53	0.49	0.41	0.56	0.46	0.36	0.33
-24	0.69	0.60	0.49	0.36	0.64	0.53	0.36	0.29
-36	0.73	0.67	0.50	0.29	0.70	0.61	0.38	0.25
-48	0.79	0.73	0.52	0.23	0.79	0.68	0.38	0.22
-72	0.88	0.83	0.71	0.28	0.88	0.82	0.62	0.25
-96	0.93	0.90	0.82	0.38	0.93	0.89	0.77	0.26
-120	0.94	0.91	0.87	0.42	0.94	0.91	0.82	0.26
-144	0.94	0.92	0.84	0.34	0.94	0.92	0.76	0.19
-168	0.95	0.92	0.46	0.19	0.94	0.89	0.44	0.11
-180	0.95	0.33	0.16	0.14	0.94	0.31	0.16	0.14

APPENDIX 5

Side force coefficients for the model fitted with vortex generators.

α (°)	$C_Y \times 10^4$					
	Vortex Generator Set No. 1	Vortex Generator Set No. 2	Vortex Generator Set No. 3	Vortex Generator Set No. 4	Vortex Generator Set No. 5	Vortex Generator Set No. 6
0.0	0.21	0.04	0.11	0.16	0.08	-0.12
4.6	-2.64	-3.78	-3.92	-3.87	-3.98	-3.39
7.6	-4.31	-5.95	-6.09	-6.29	-6.23	-5.68
12.3	-7.59	-9.32	-10.01	-10.65	-10.32	-9.35
17.0	-11.04	-13.21	-13.74	-14.52	-14.97	-14.35
21.9	-15.22	-17.75	-17.52	-18.80	-19.53	-18.30
28.6	-20.60	-23.57	-23.57	-24.10	-25.21	-23.84
-4.6	3.00	3.56	3.14	4.31	3.59	3.37
-7.6	4.84	5.23	6.18	6.57	6.43	6.09
-12.3	8.15	8.76	10.21	10.18	11.02	10.26
-17.0	11.40	12.41	14.52	13.80	14.97	14.80
-21.9	15.77	16.69	18.16	17.77	17.61	18.50
-28.6	21.24	22.47	24.31	23.26	23.26	24.12

APPENDIX 6

Resistance coefficients for the model fitted with vortex generators.

Vortex Generator Set No. 1		Vortex Generator Set No. 2		Vortex Generator Set No.3	
$R_N \times 10^{-6}$	$C_D \times 10^3$	$R_N \times 10^{-6}$	$C_D \times 10^3$	$R_N \times 10^{-6}$	$C_D \times 10^3$
8.16	4.03	8.23	3.99	7.89	3.98
8.82	3.97	8.90	3.95	8.48	3.95
9.49	3.93	9.45	3.91	9.07	3.93
10.02	3.90	10.08	3.88	9.61	3.91
9.75	3.92	9.77	3.89	9.79	3.88
9.15	3.95	9.80	3.89	9.21	3.93
8.56	3.99	9.17	3.93	8.57	3.96
		8.53	3.98		
		7.83	4.02		

Vortex Generator Set No. 4		Vortex Generator Set No. 5		Vortex Generator Set No. 6	
$R_N \times 10^{-6}$	$C_D \times 10^3$	$R_N \times 10^{-6}$	$C_D \times 10^3$	$R_N \times 10^{-6}$	$C_D \times 10^3$
8.04	4.01	7.80	3.97	7.86	4.02
8.67	3.95	8.44	3.94	8.49	3.97
9.25	3.91	9.01	3.90	9.09	3.93
9.84	3.92	9.59	3.89	9.65	3.88
9.57	3.92	9.28	3.90	9.33	3.90
8.99	3.95	8.72	3.93	8.80	3.95
8.37	3.96	8.18	3.97	8.22	4.00

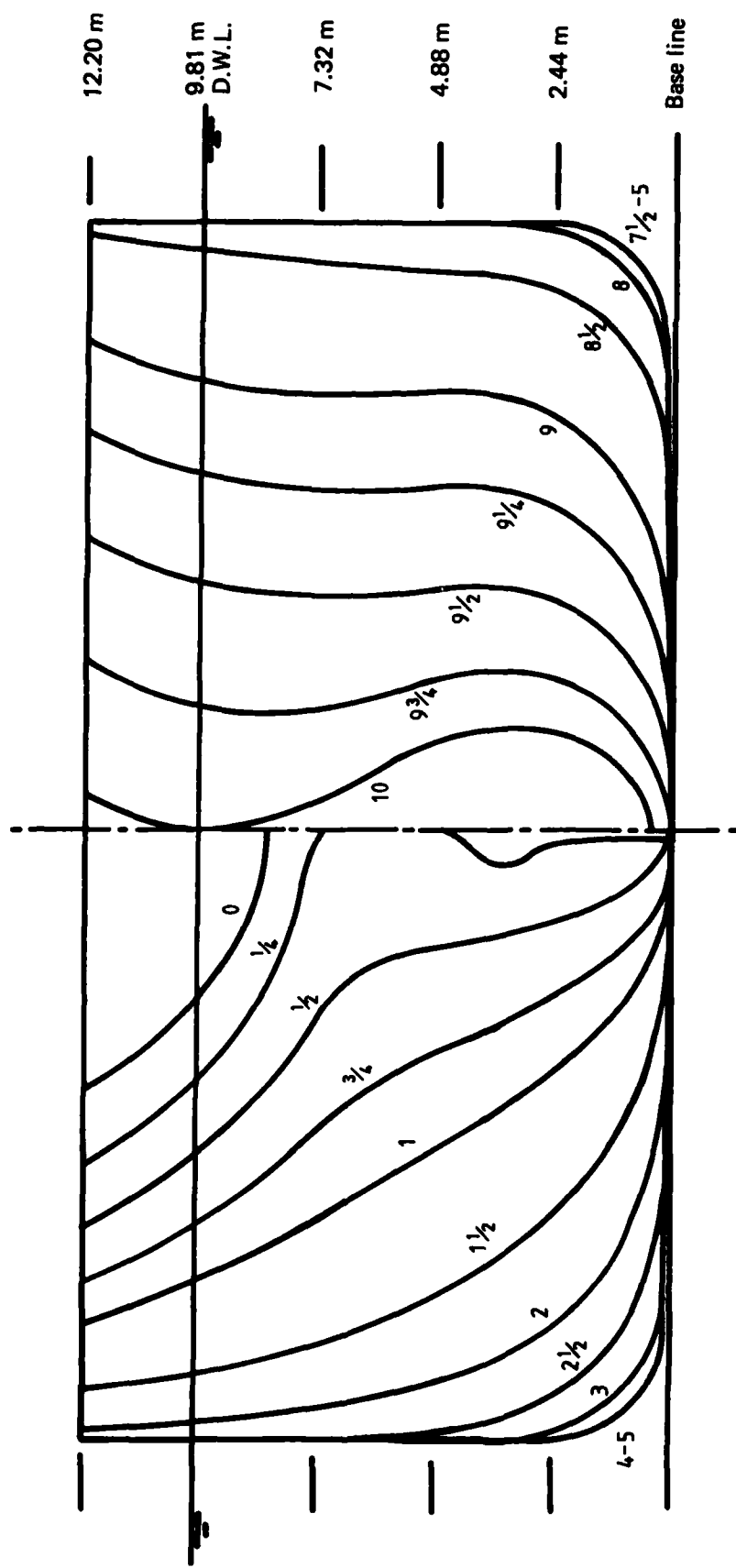


FIG. 1. SHIP SECTION LINES

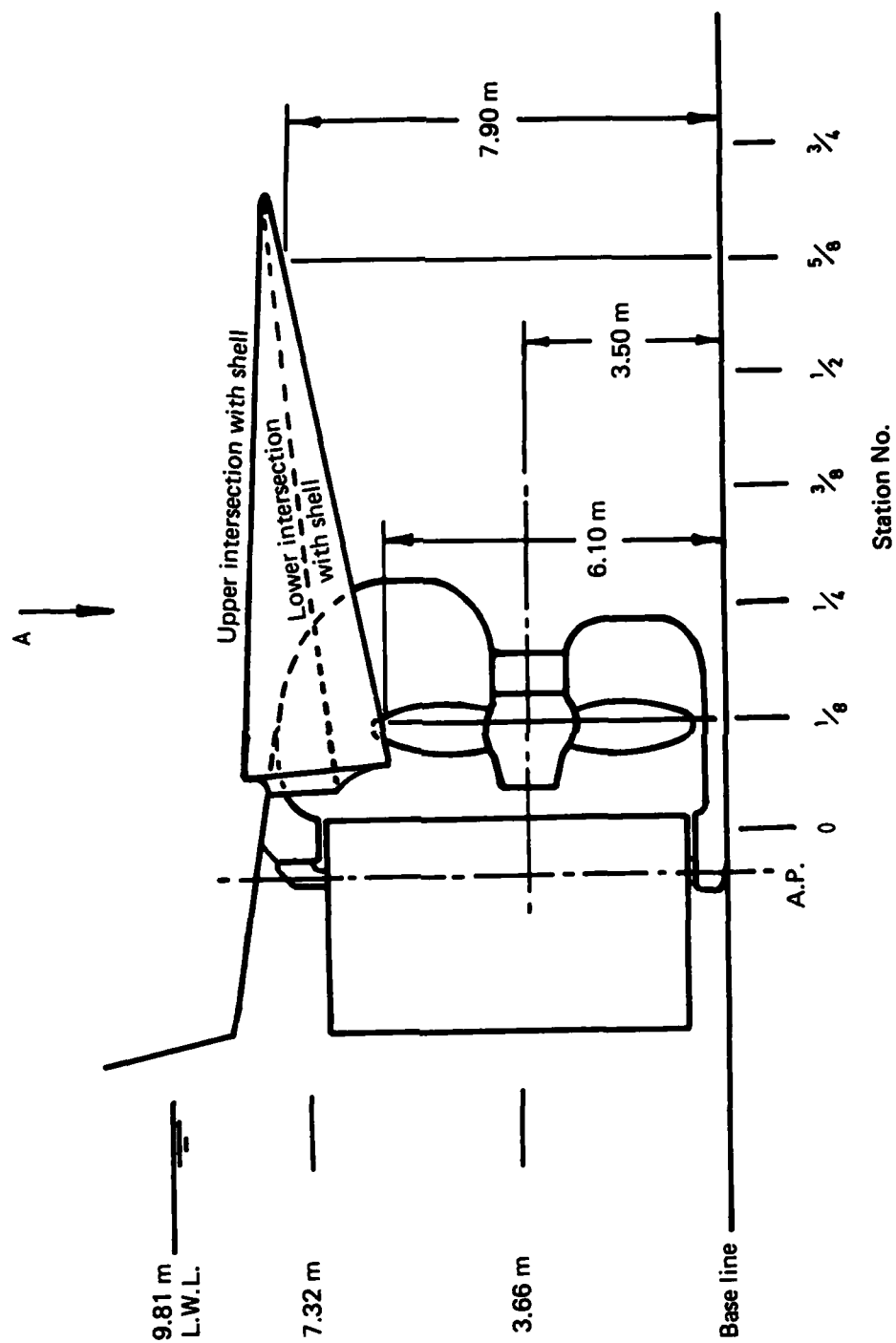


FIG. 2. STERN ARRANGEMENT

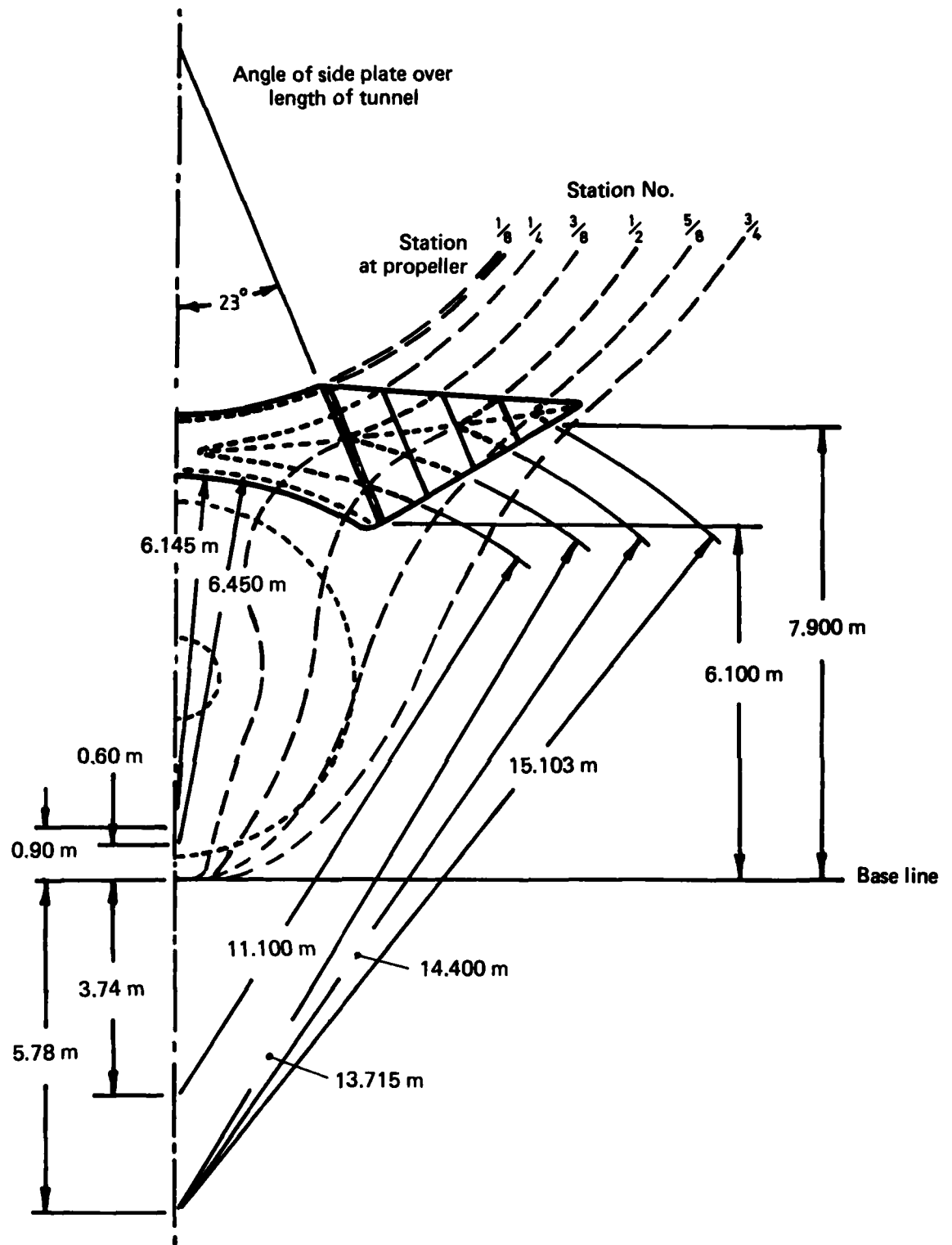
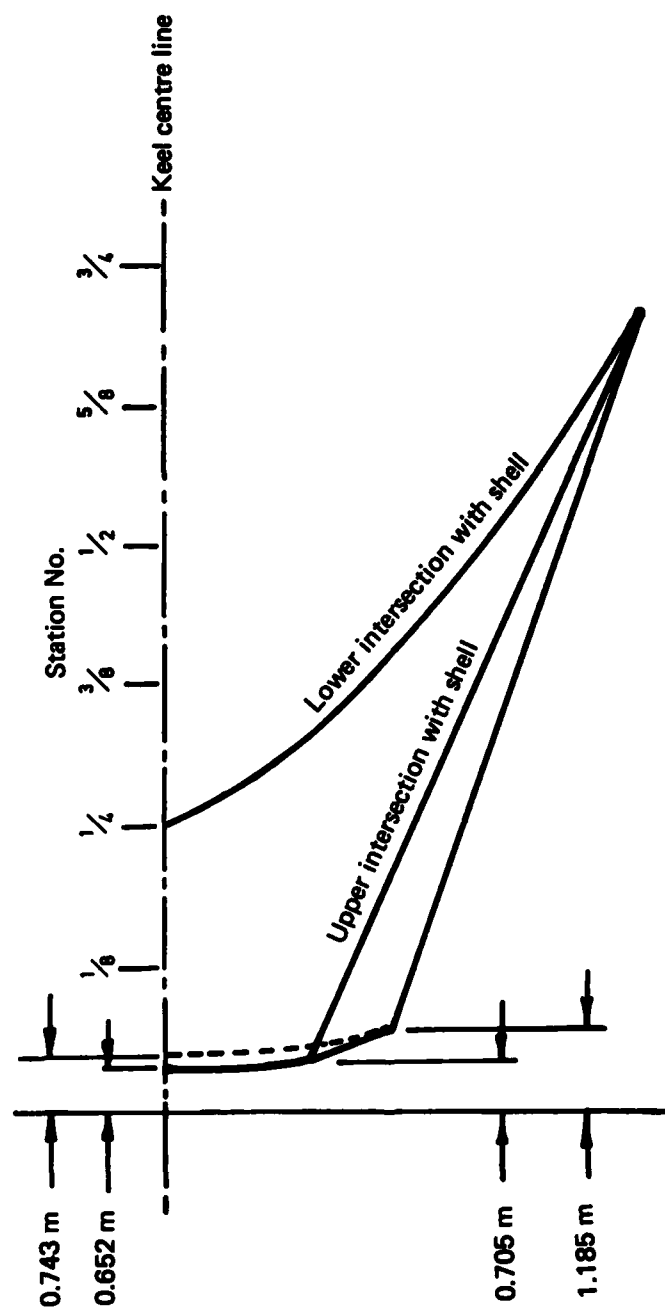


FIG. 3. PROPELLER TUNNEL
(a) Tunnel offsets



View A on Fig. 2

Fig. 3 (cont)
(b) Plan of propeller tunnel

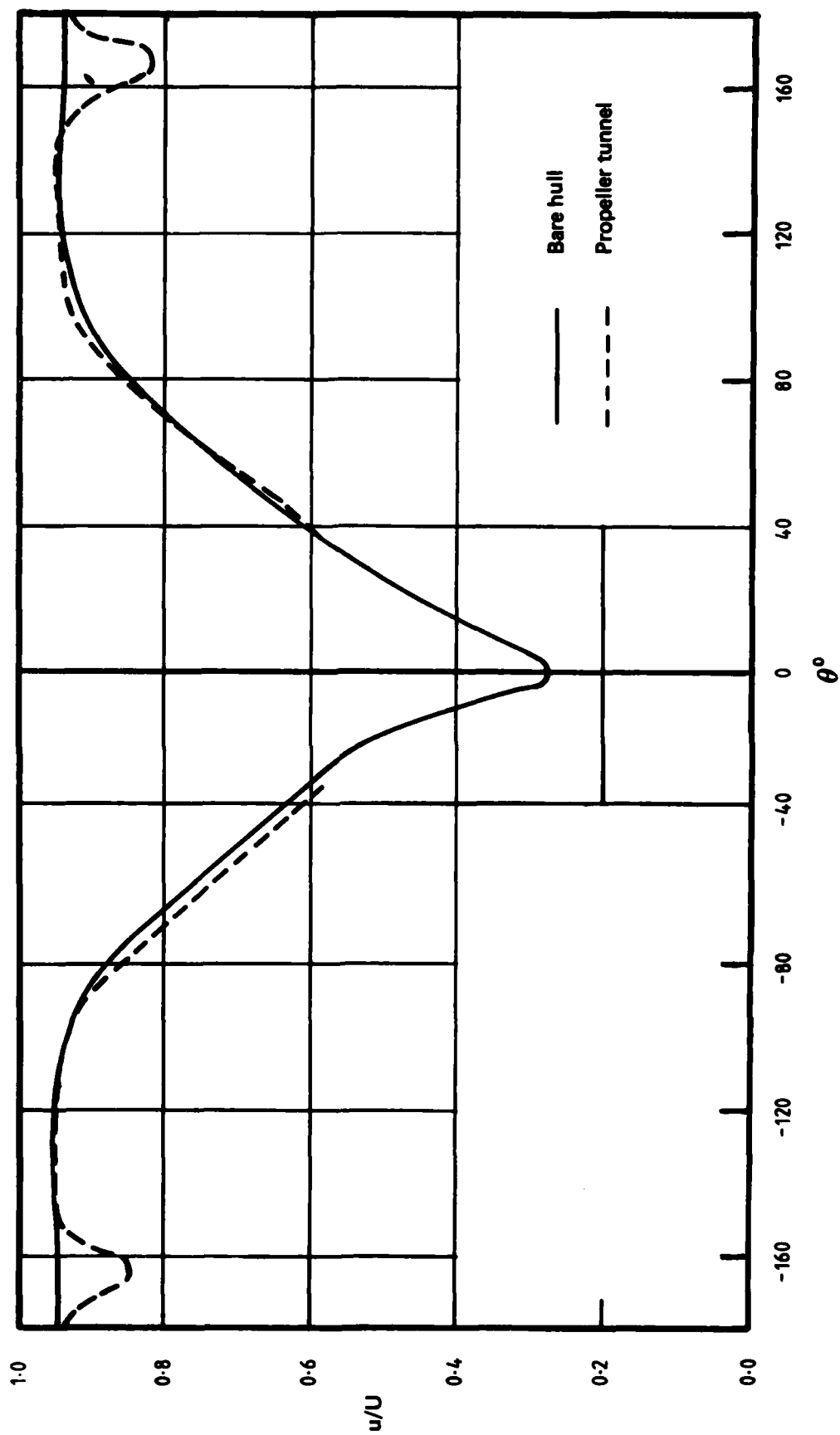


FIG. 4. AXIAL VELOCITY DISTRIBUTION OF THE FLOW IN THE PROPELLER PLANE OF THE MODEL
(a) $r/R = 1.23$

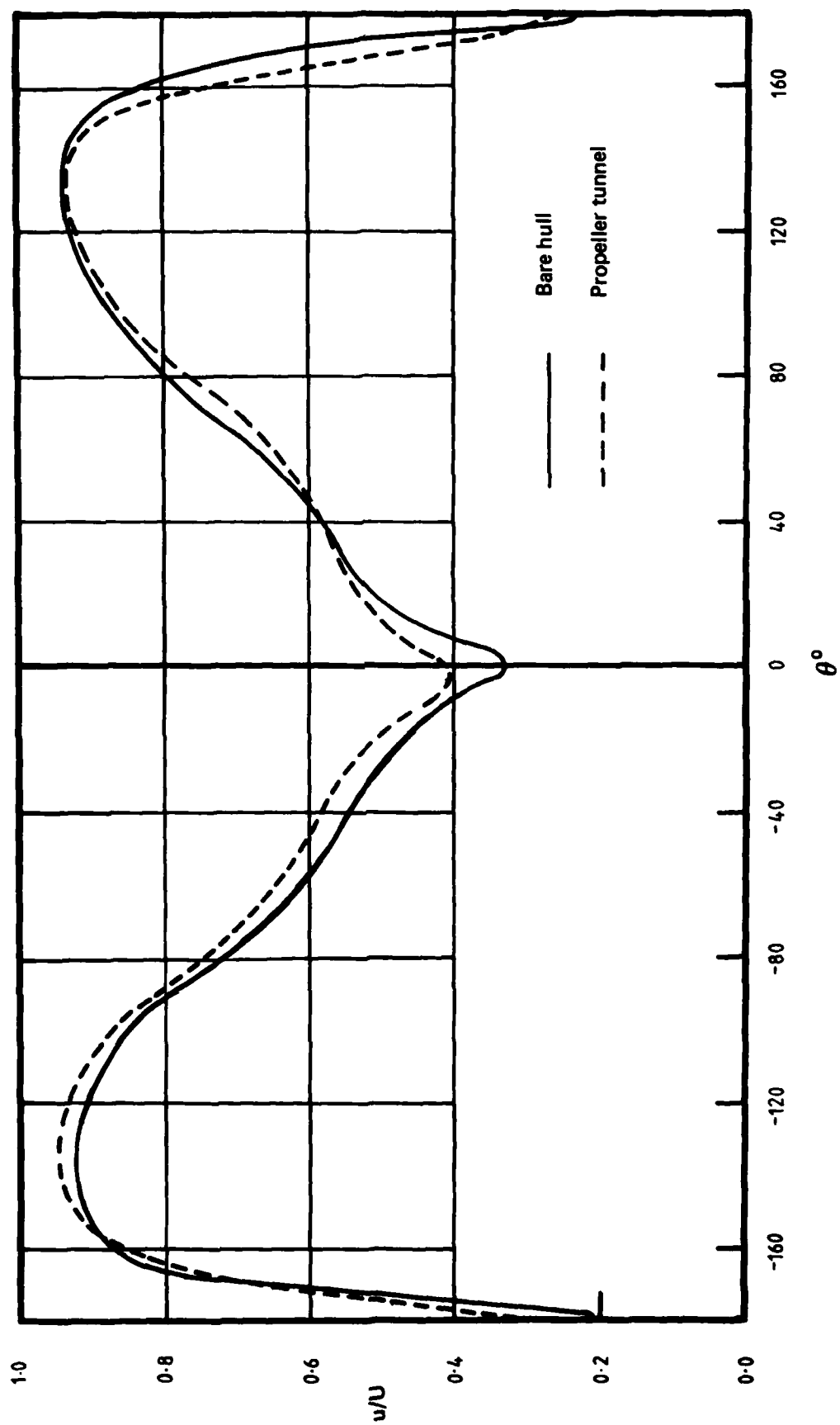


Fig. 4 (cont)
(b) $r/R = 0.96$

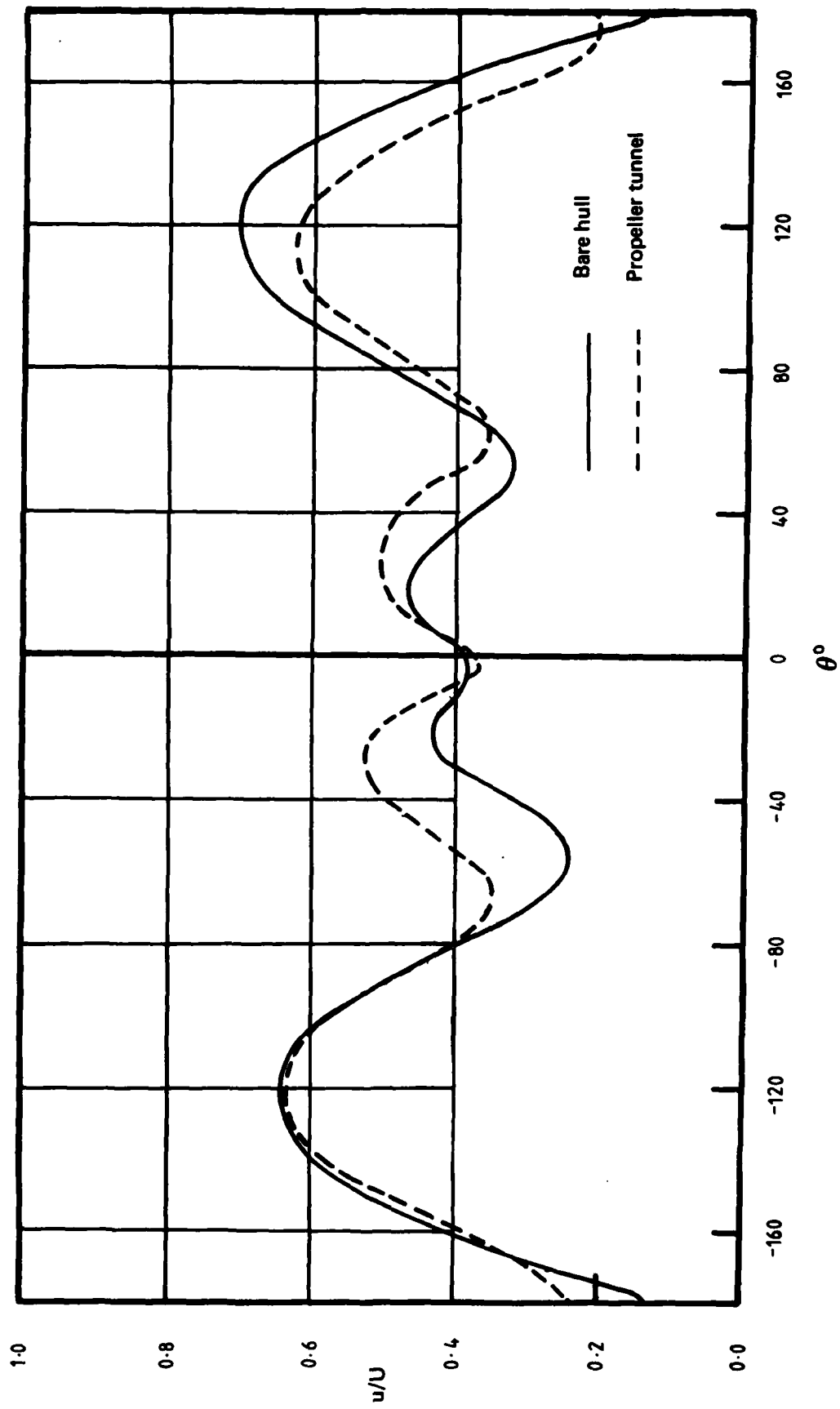


Fig. 4 (cont)
(c) $r/R = 0.68$

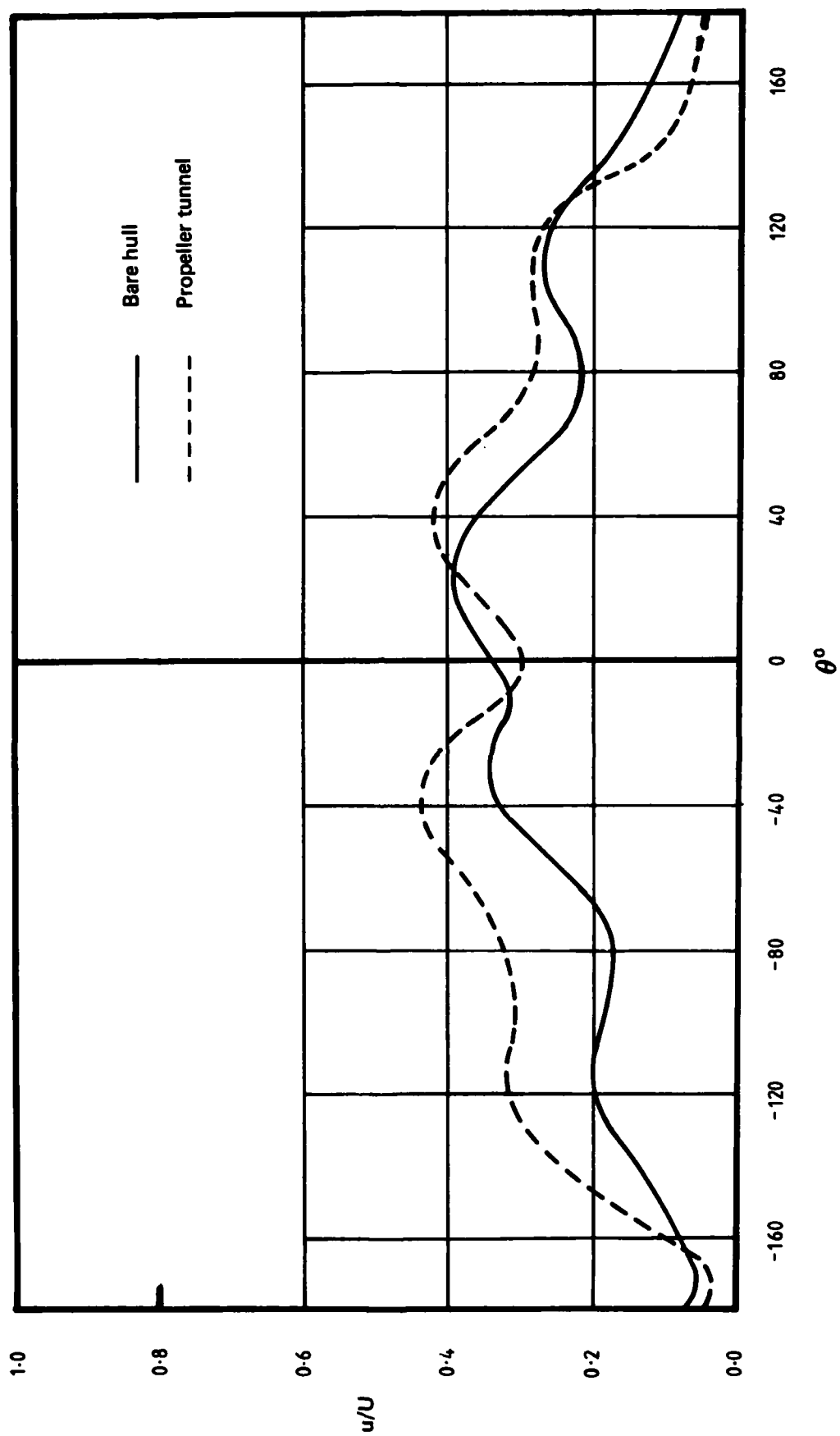


Fig. 4 (cont)
(d) $r/R = 0.41$



FIG. 5. FLOW PATTERN OVER THE STERN OF THE MODEL

(a) Bare hull



Fig. 5 (cont)
(b) Model fitted with propeller tunnel

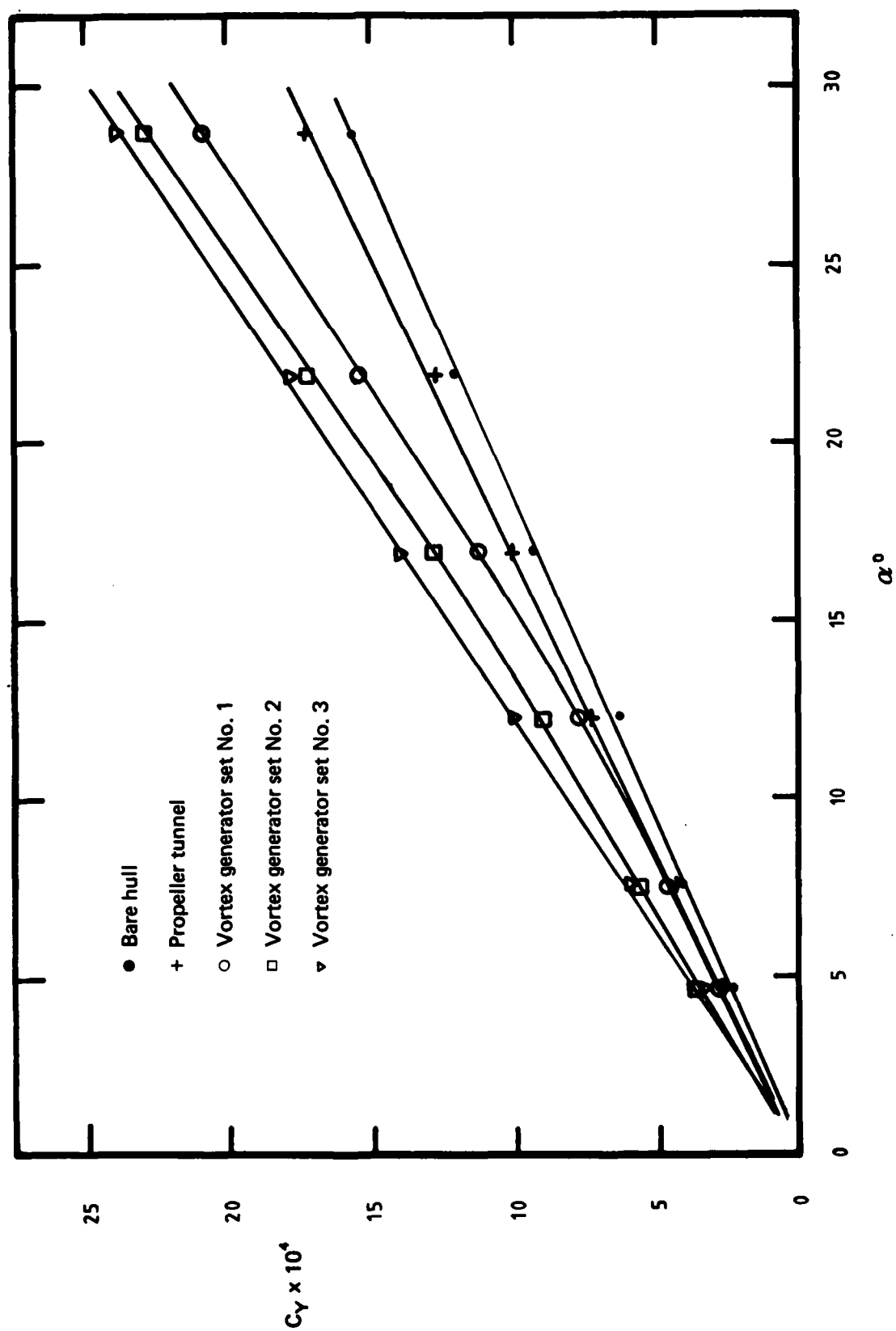


FIG. 6. SIDE FORCE COEFFICIENTS FOR THE MODEL

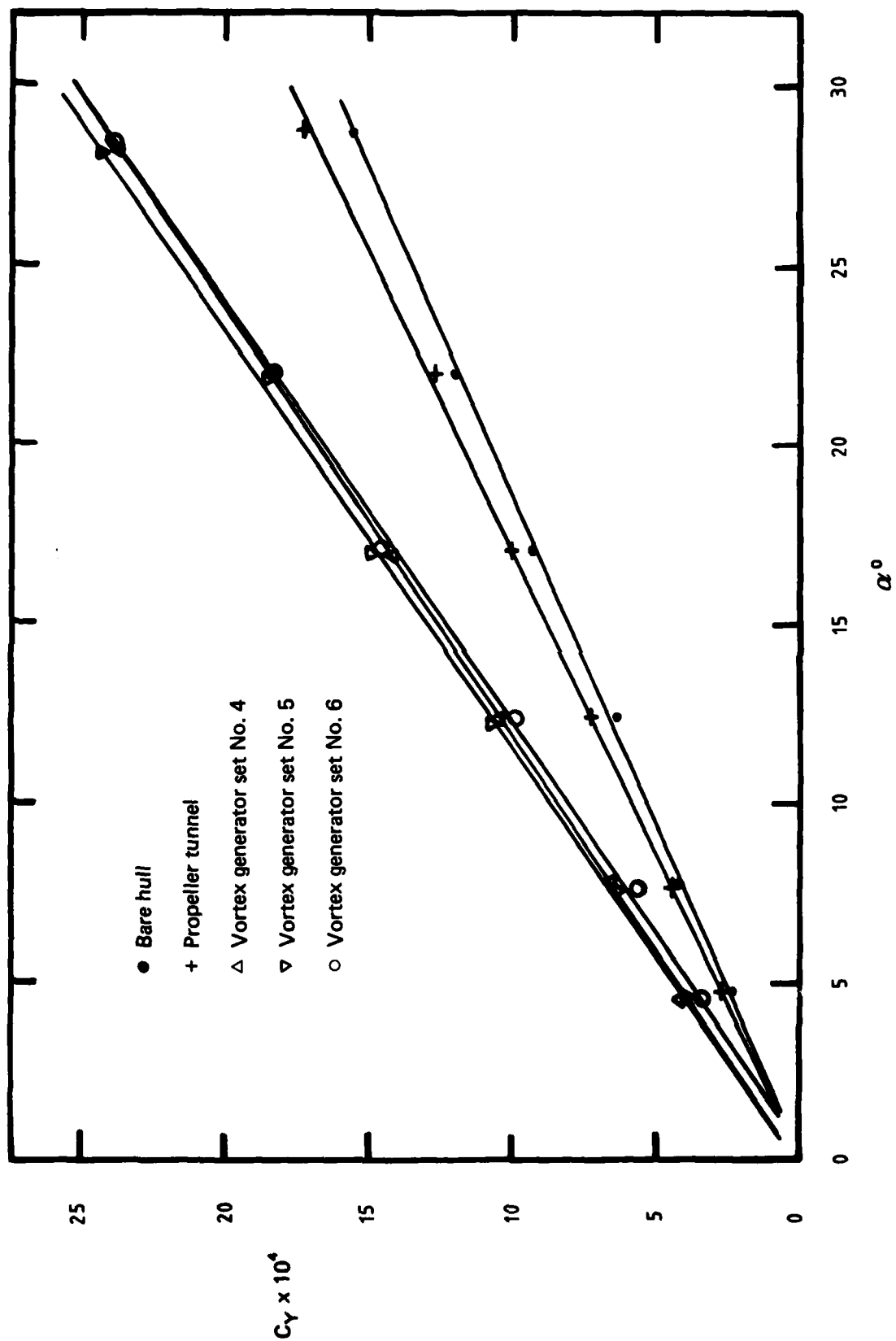


Fig. 6 (cont)

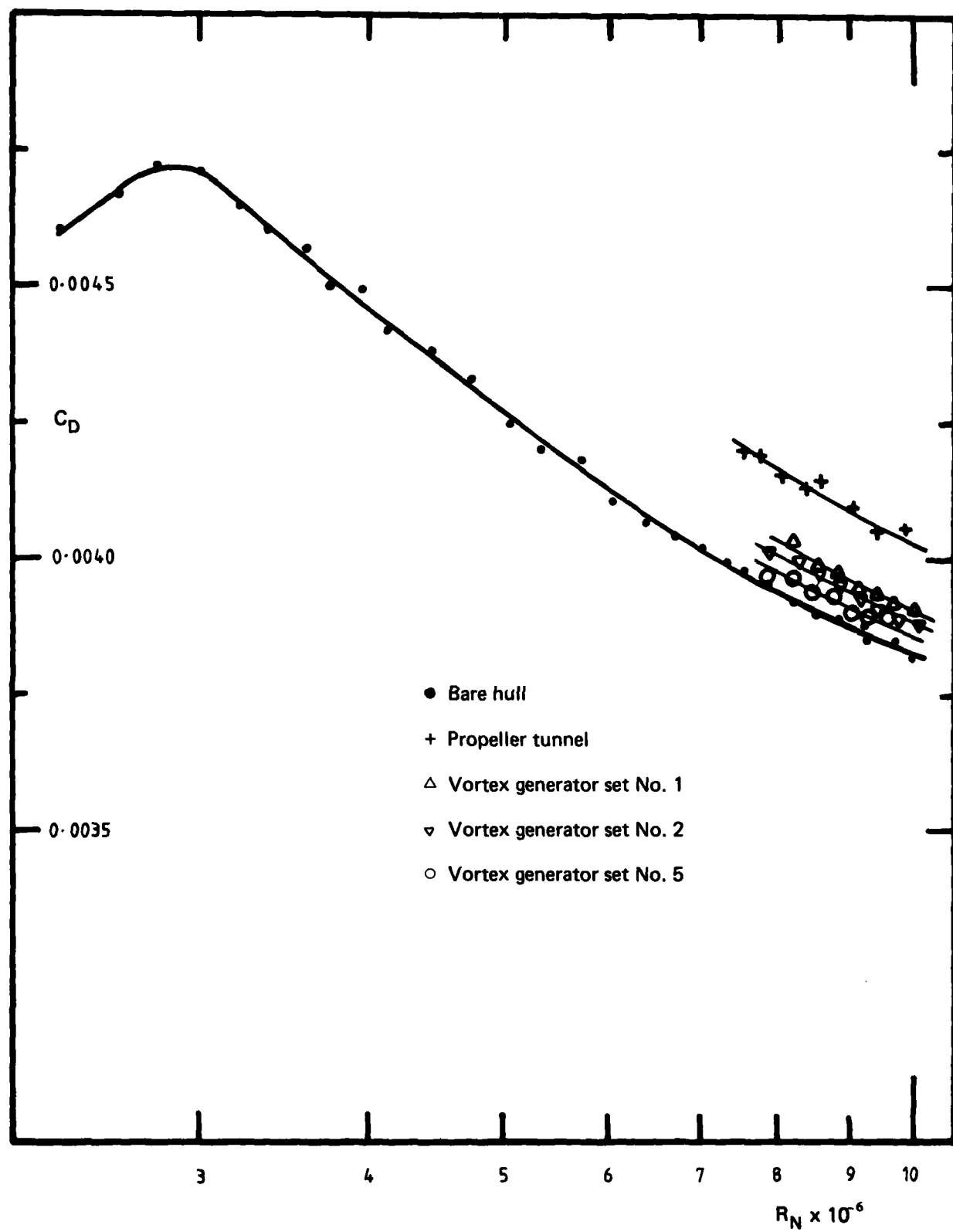


FIG. 7. RESISTANCE COEFFICIENTS

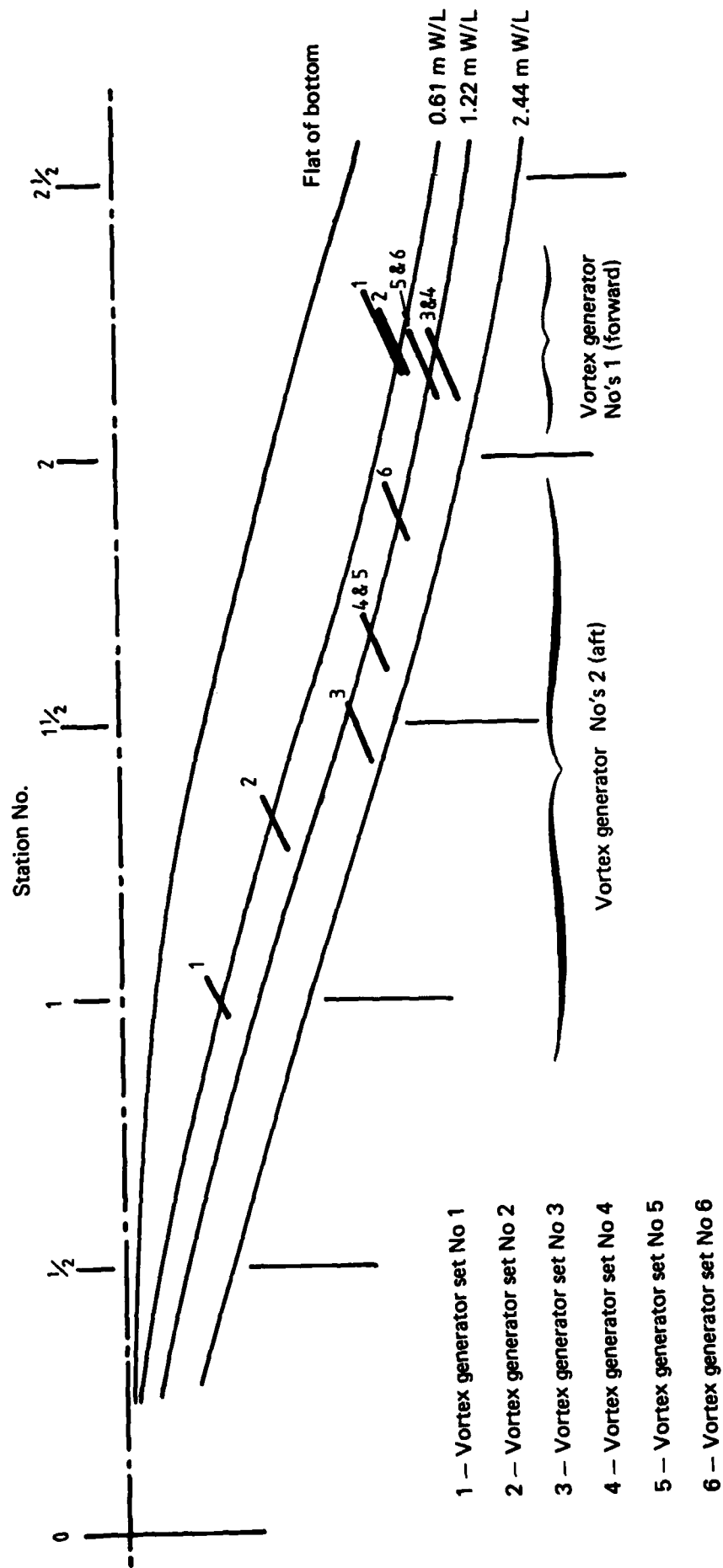


FIG. 8. LOCATION OF THE VORTEX GENERATORS

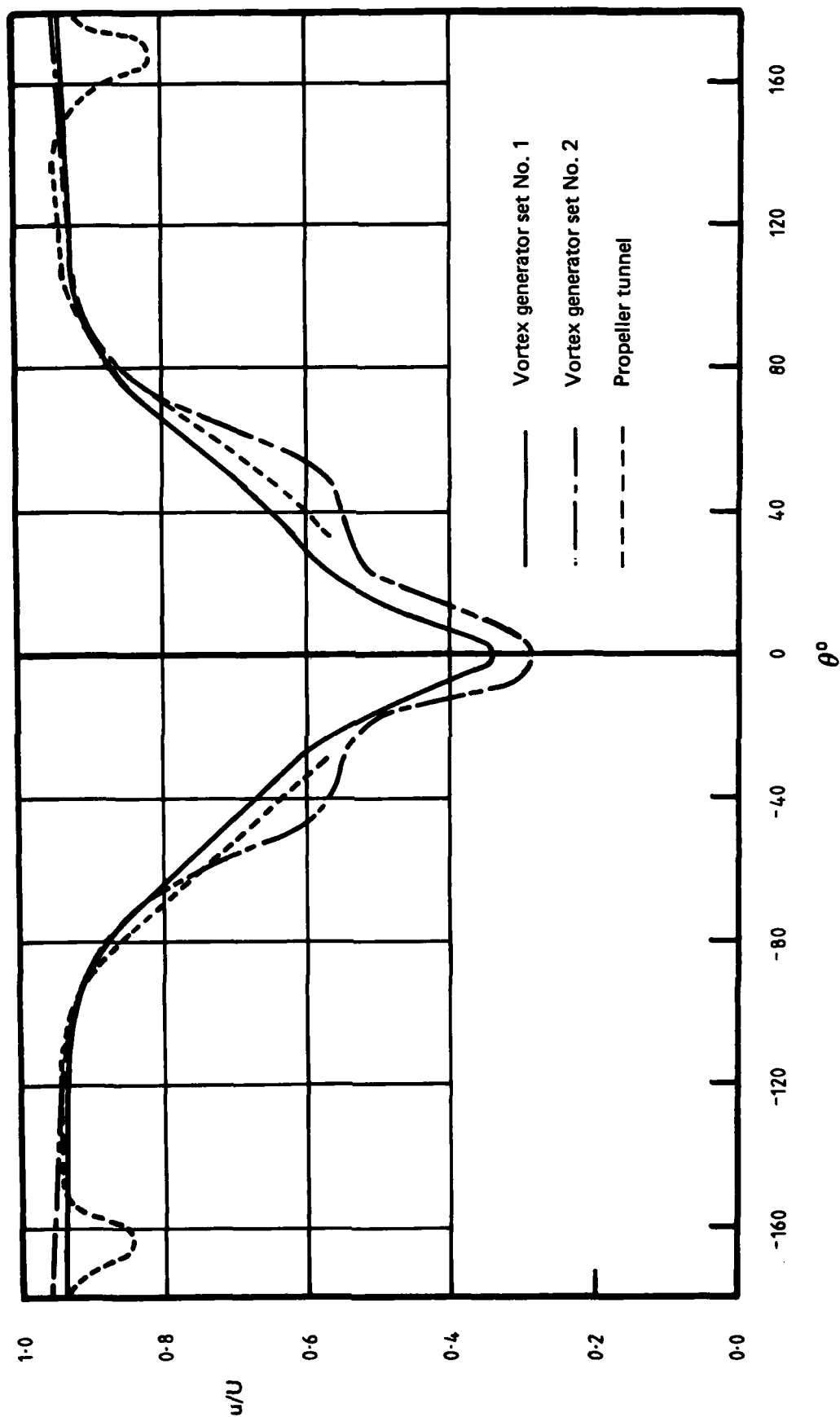


FIG. 9. AXIAL VELOCITY DISTRIBUTION OF THE FLOW IN THE PROPELLER PLANE OF THE MODEL FITTED WITH VORTEX GENERATOR SET NO. 1, AND SET NO. 2.

(a) $r/R = 1.23$

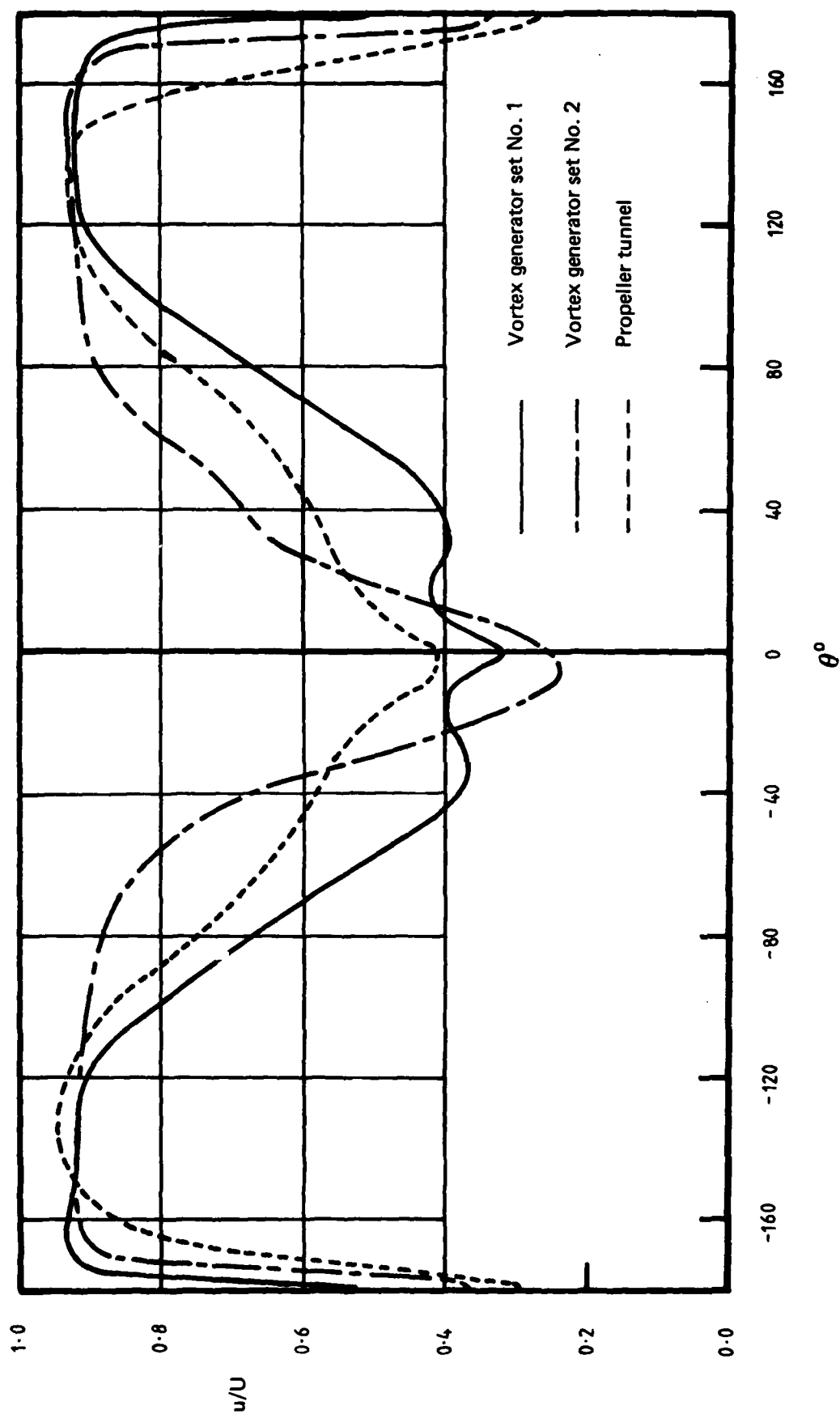


Fig. 9 (cont)
(b) $r/R = 0.96$

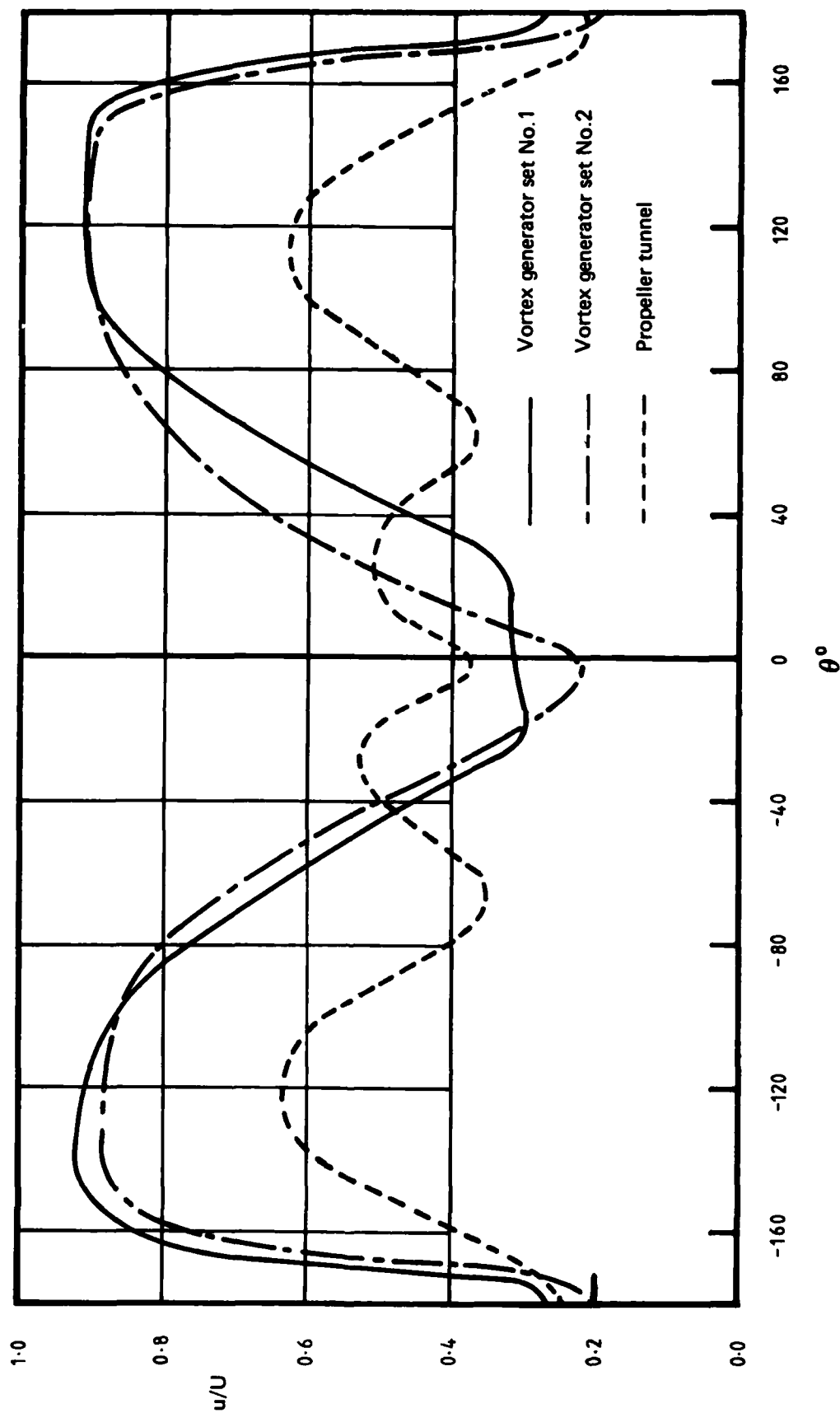


Fig. 9 (cont)
(c) $r/R = 0.68$

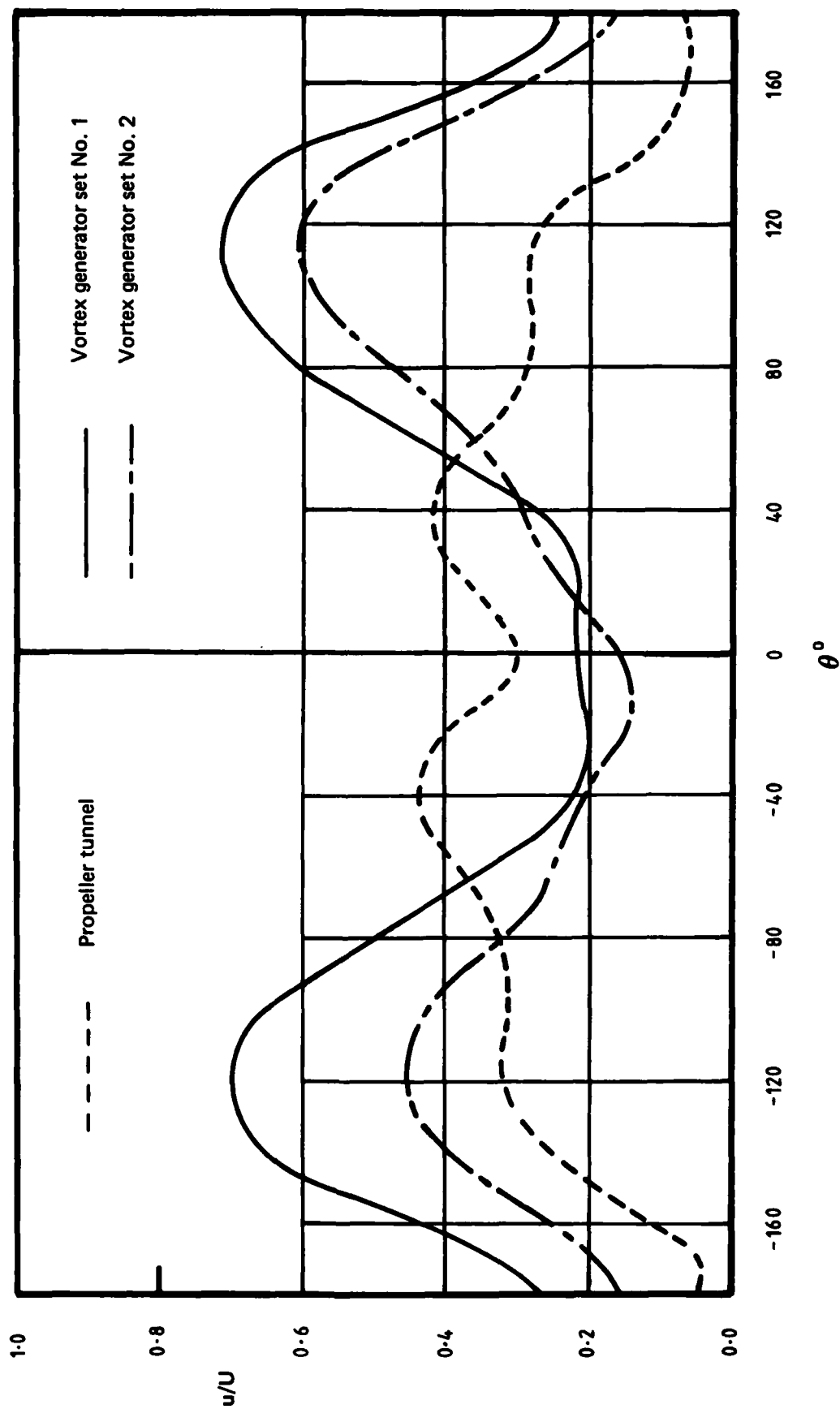


Fig 9 (cont)
(d) $r/R = 0.41$



FIG. 10. FLOW PATTERN OVER THE STERN OF THE MODEL FITTED WITH VORTEX GENERATOR SET NO. 1.



FIG. 11. FLOW PATTERN OVER THE STERN OF THE MODEL FITTED WITH VORTEX GENERATOR SET NO. 2.

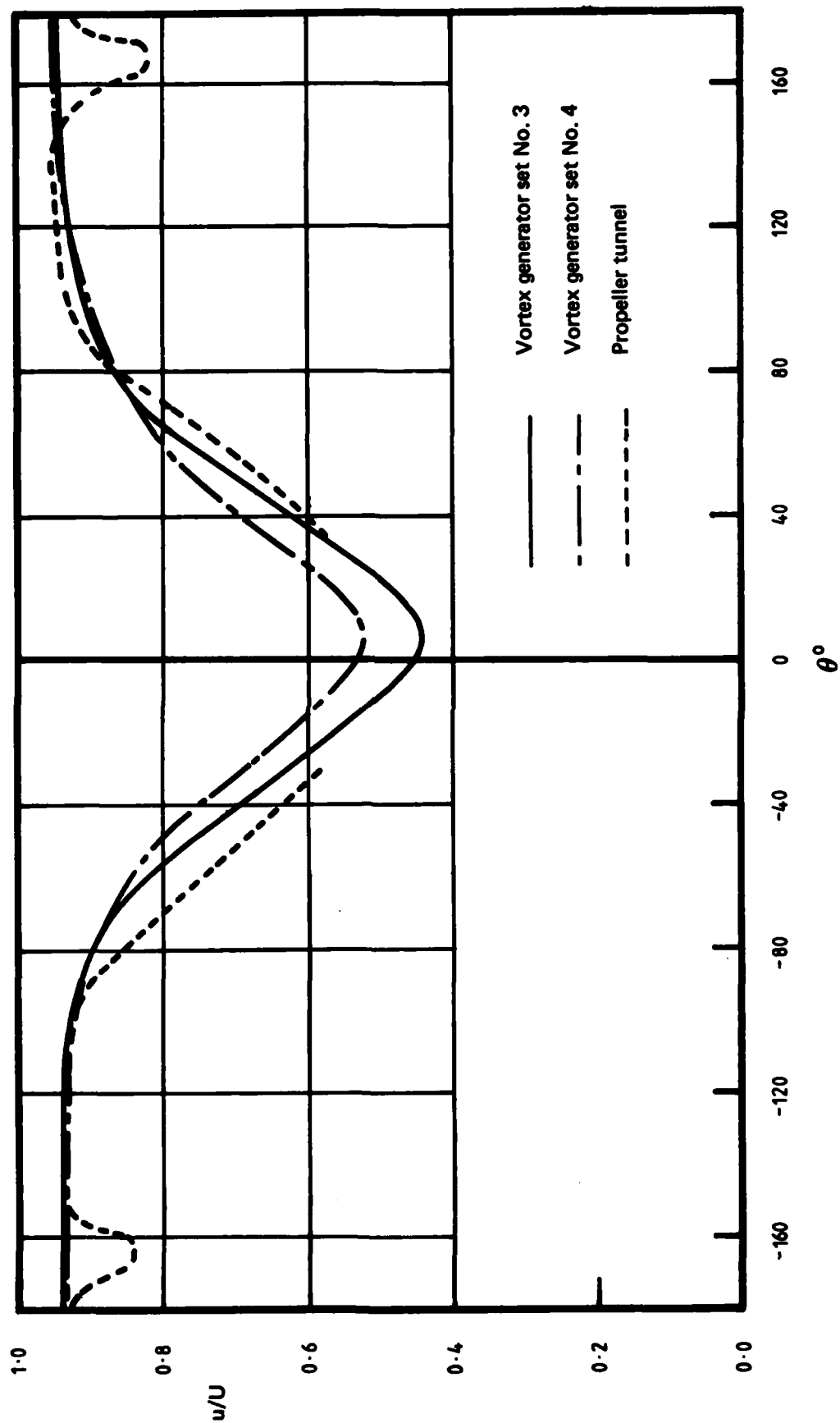


FIG 12. AXIAL VELOCITY DISTRIBUTION OF THE FLOW IN THE PROPELLER PLANE OF THE MODEL FITTED WITH VORTEX GENERATOR SET NO. 3, AND SET NO. 4.

(a) $r/R = 1.23$

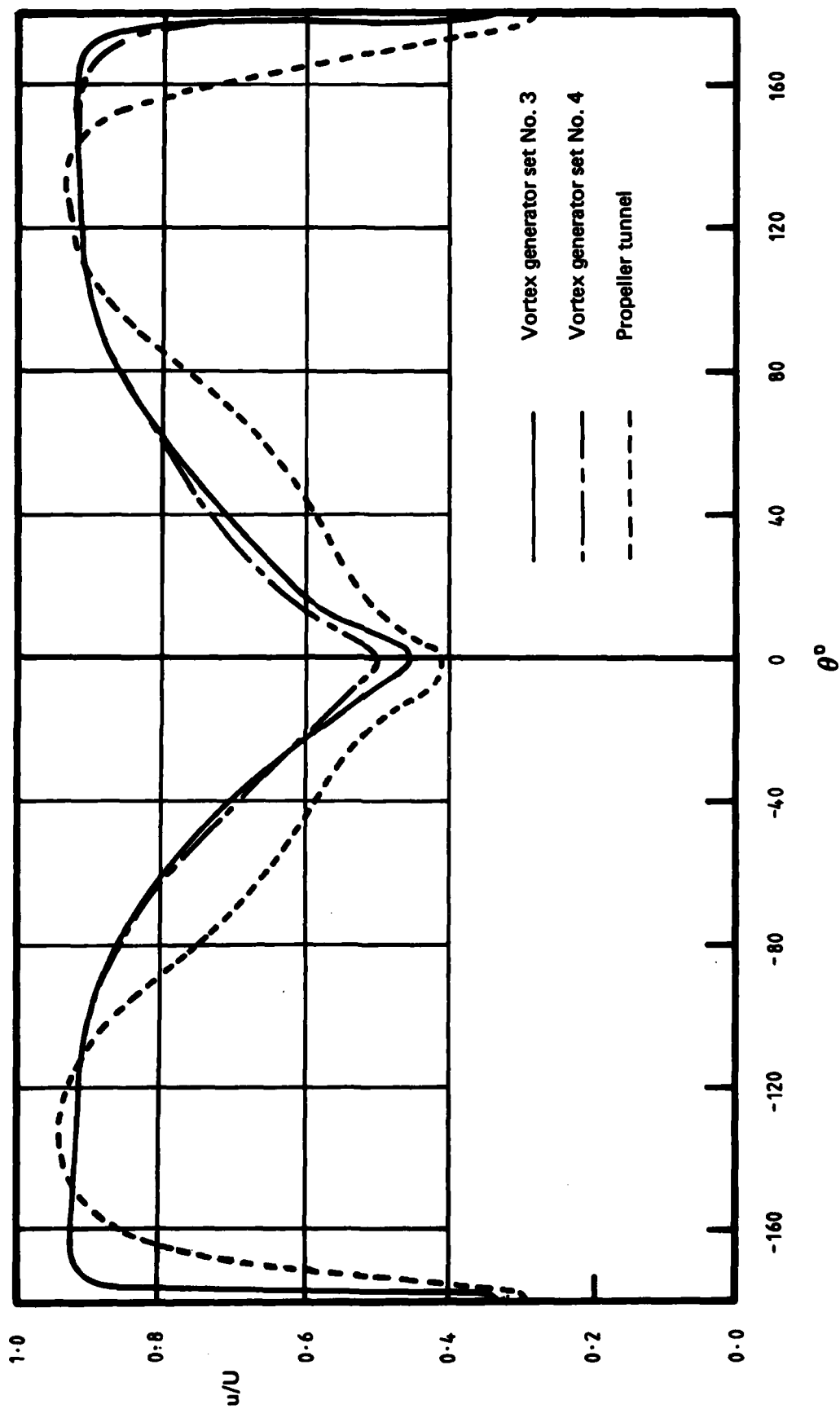


Fig. 12 (cont)
(b) $r/R = 0.96$

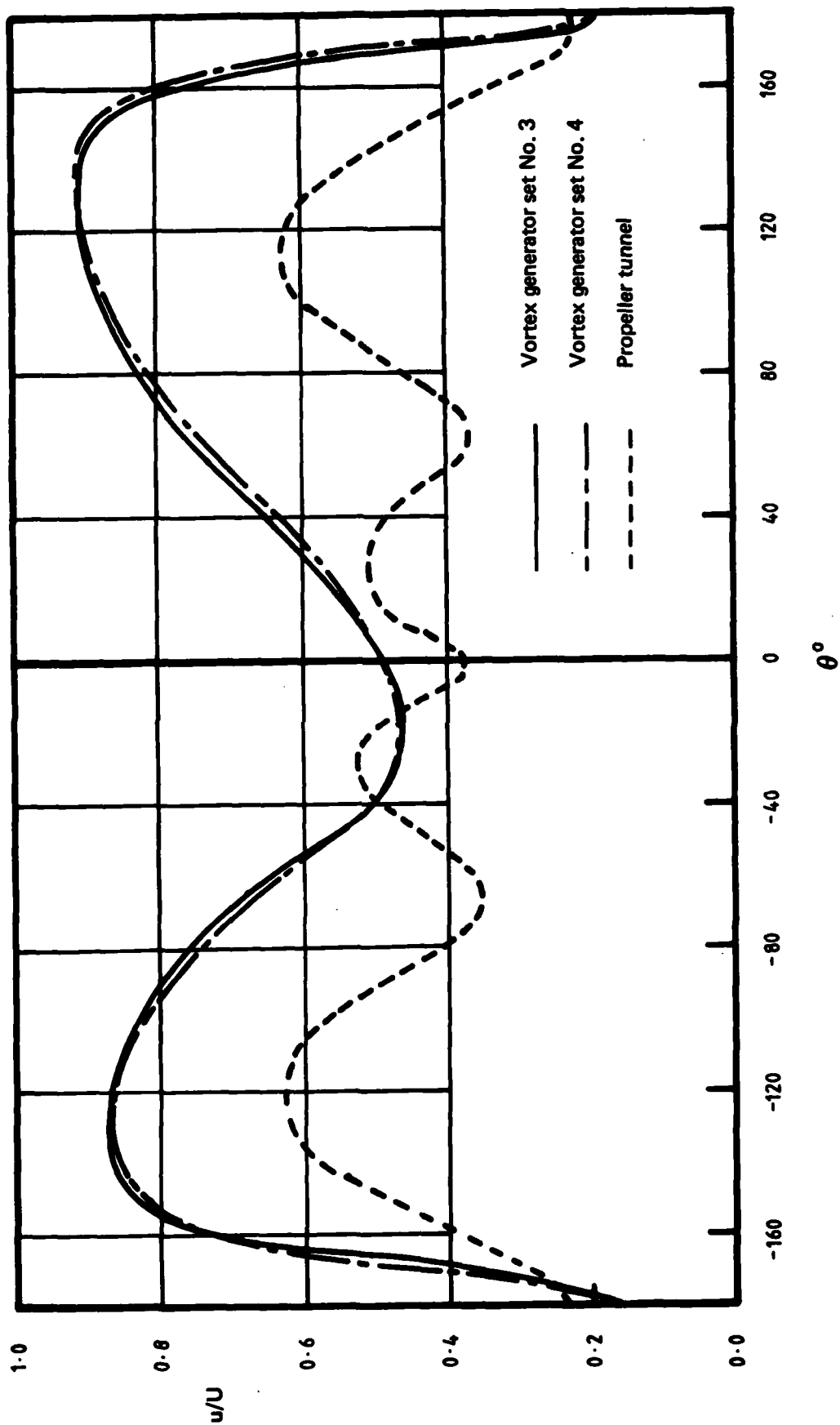


Fig. 12 (cont)
(c) $r/R = 0.68$

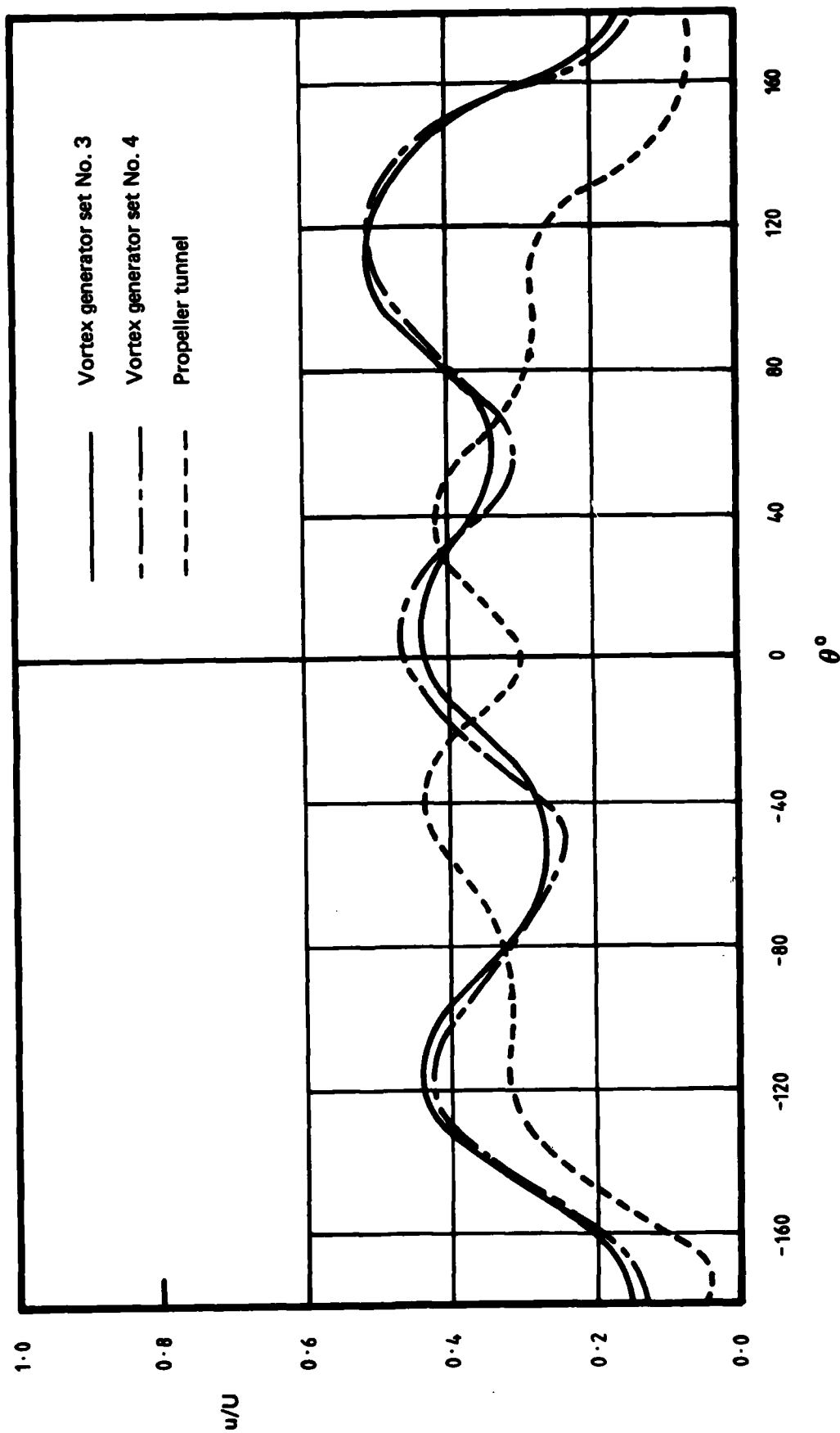


Fig. 12 (cont)
(d) $r/R = 0.41$

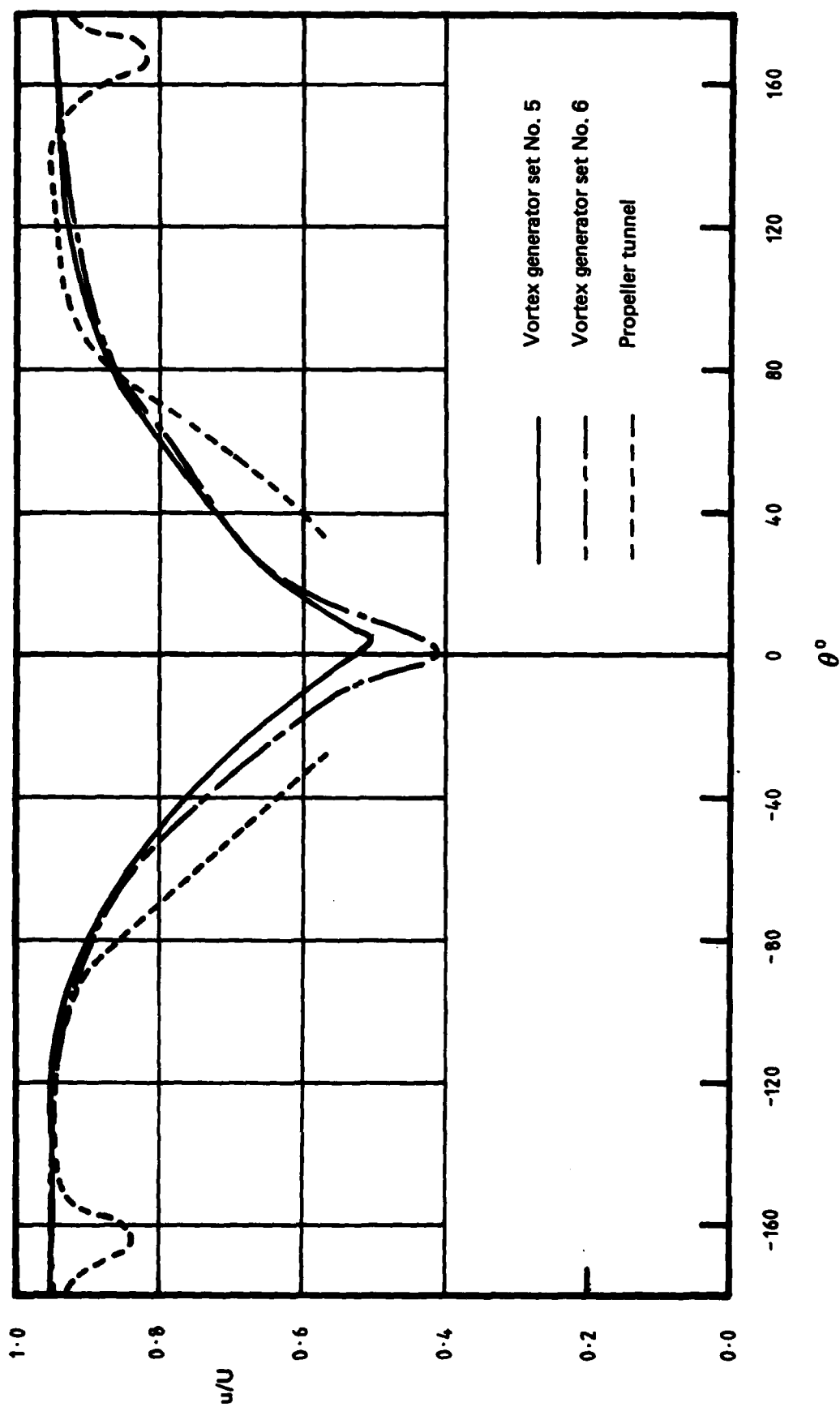


FIG. 13. AXIAL VELOCITY DISTRIBUTION OF THE FLOW IN THE PROPELLER PLANE OF THE MODEL FITTED WITH VORTEX GENERATOR SET NO. 5, AND SET NO. 6.
(a) $r/R = 1.23$

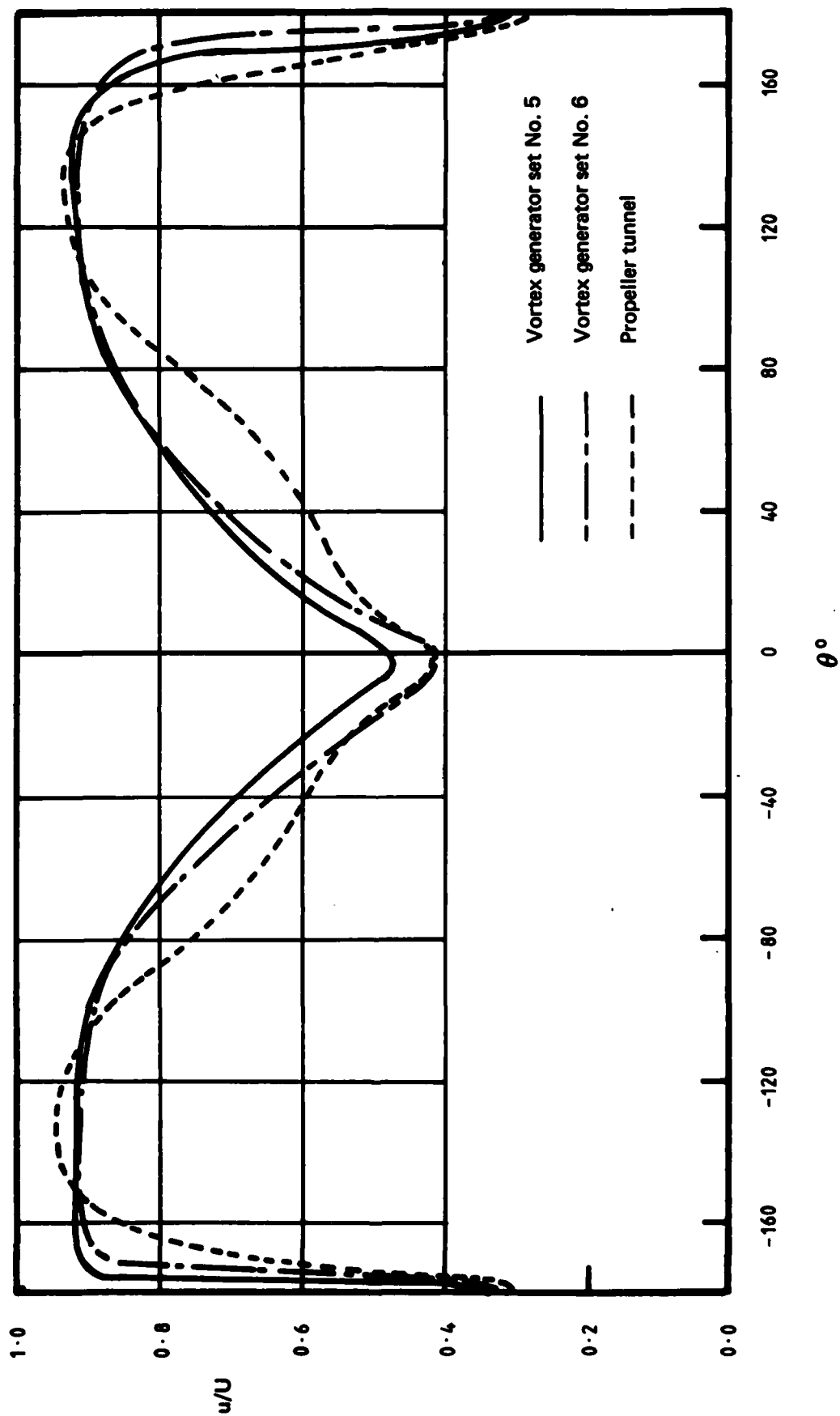


Fig. 13 (cont)
(b) $r/R = 0.96$

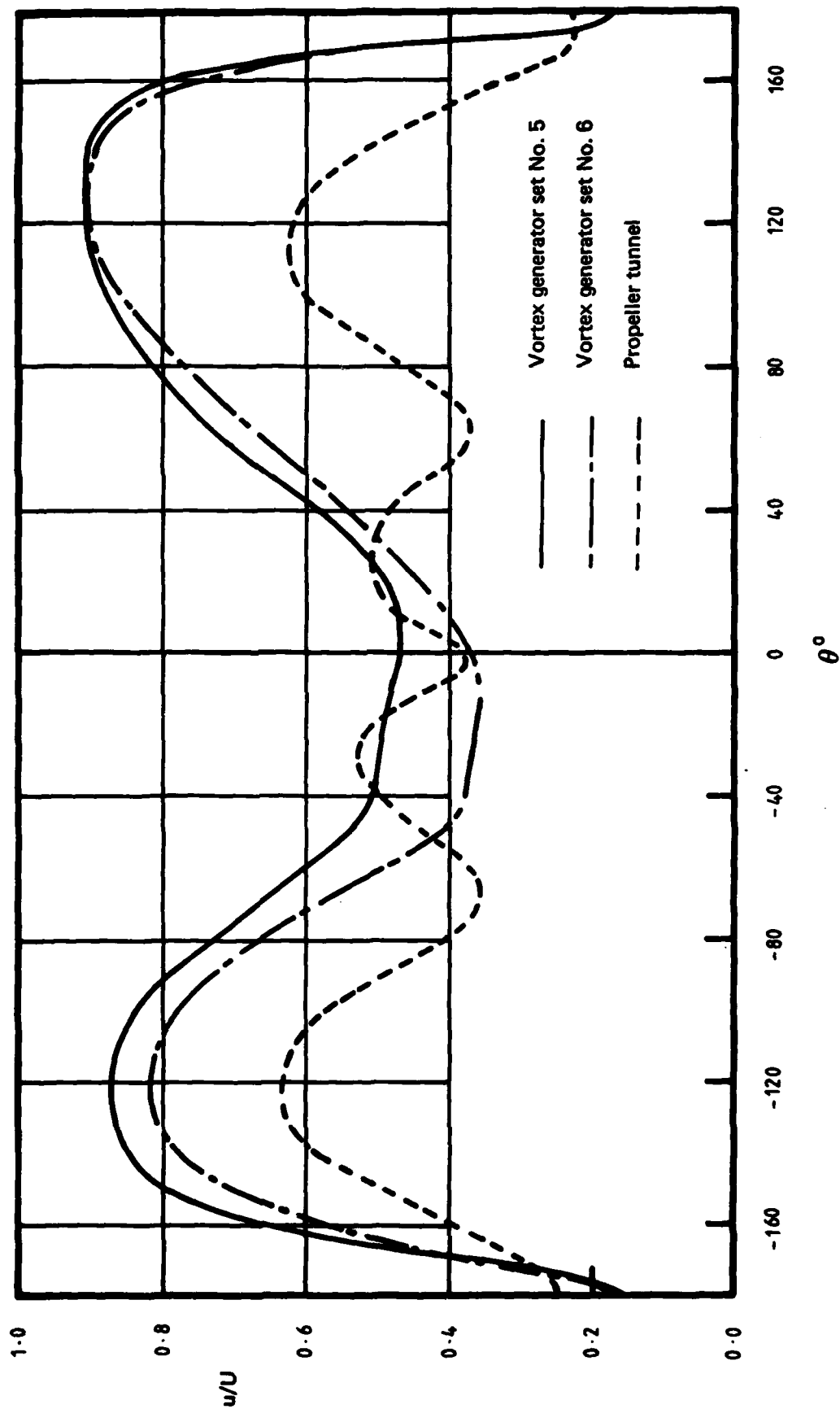


Fig. 13 (cont)
(c) $r/R = 0.68$

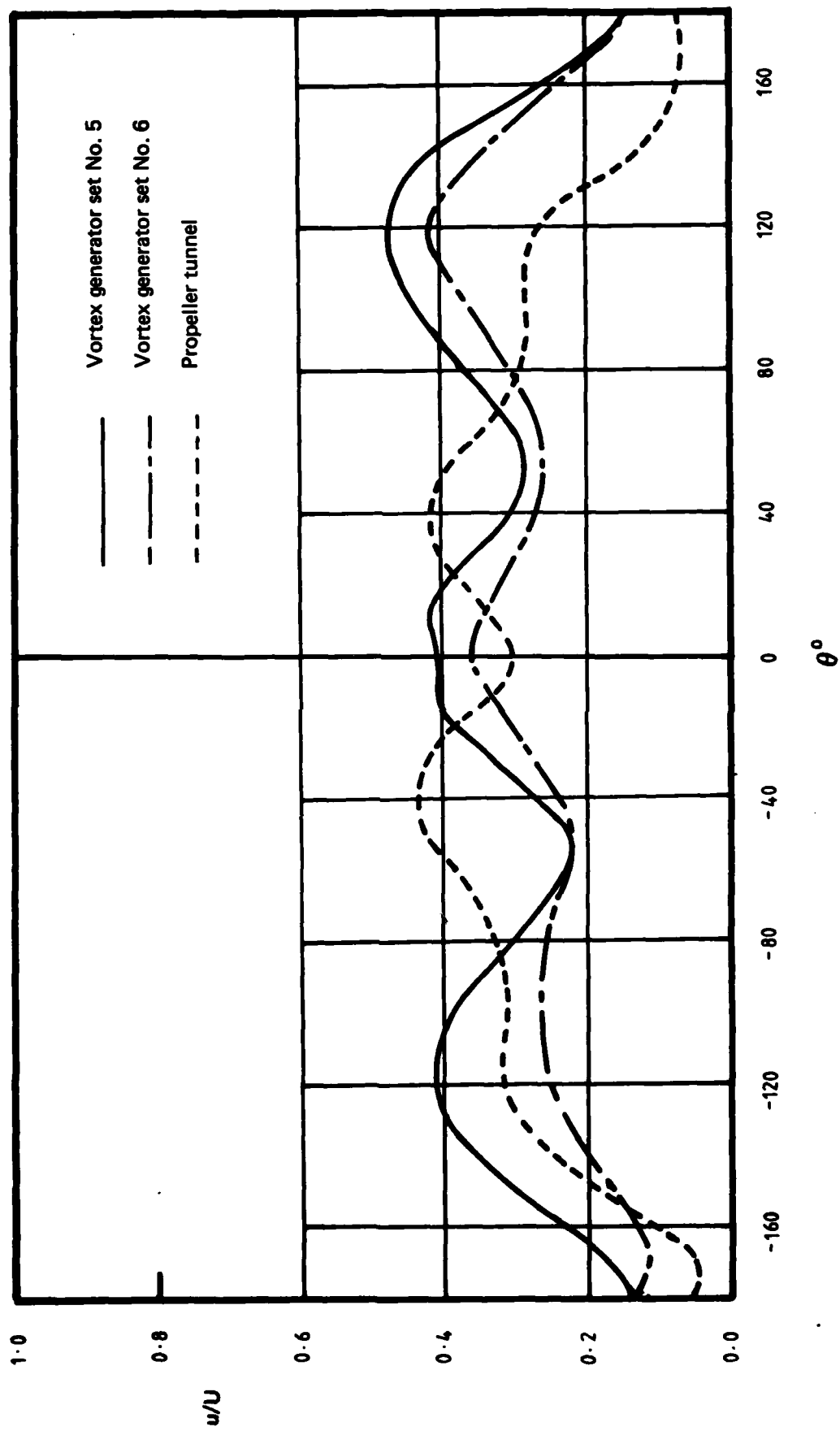


Fig. 13 (cont)
(d) $r/R = 0.41$



FIG. 14. FLOW PATTERN OVER THE STERN OF THE MODEL FITTED WITH VORTEX GENERATOR SET No. 5.

DISTRIBUTION

AUSTRALIA

COPY NO.

DEPARTMENT OF DEFENCE

Central Office

Chief Defence Scientist	1
Deputy Chief Defence Scientist	2
Superintendent, Science and Technology Programs	3
Australian Defence Scientific and Technical Representative (UK)	4
Counsellor, Defence Science (USA)	5
Defence Library	6
Assistant Secretary, D.I.S.B.	7-22
Joint Intelligence Organisation	23

Aeronautical Research Laboratories

Chief Superintendent	24
Library	25
Superintendent, Aerodynamics Division	26
Divisional File, Aerodynamics Division	27
N. Matheson	28

Materials Research Laboratories

Library	29
---------	----

Defence Research Centre, Salisbury

Library	30
---------	----

RAN Research Laboratory

Library	31
---------	----

Navy Office

Naval Scientific Adviser	32
--------------------------	----

Department of Industry and Commerce

Superintendent, Ship Design Group	33
-----------------------------------	----

Department of Transport

Secretary	34
-----------	----

Statutory, State Authorities and Industry

ANL, Superintendent New Construction	35
ANL, Technical Director	36
Ampol Petroleum Pty. Ltd., Engineering Superintendent	37
B.P. Australia	38
Esso Research Laboratories, Director	39
Shell Co. of Australia, Library	40
H. C. Sleight Ltd., Technical Department Library	41

Universities and Colleges

Adelaide	Barr Smith Library	42
Australian National	Library	43
Melbourne	Engineering Library	44
Monash	Library	45
Sydney	Engineering Library	46
New South Wales	Physical Sciences Library	47
Queensland	Library	48

Tasmania	Engineering Library	49
West. Australian	Library	50
R.M.I.T.	Library	51
CANADA		
Marine Dynamics and Ship Laboratory		52
FRANCE		
AGARD, Library		53
ONERA, Library		54
Service de Documentation, Technique de l'Aeronautique		55
GERMANY		
Hamburg Ship Model Basin (HSVA)		56
Hamburgische Schiffbau-Versuchsanstalt		57
Institute fur Schiffbau der Universitat Hamburg		58
INDIA		
Indian Institute of Technology, Library		59
ITALY		
Instituto Nazionale per Studi ed Esperienze de Architettura Navale		60
JAPAN		
Ship Research Institute		61
Shipbuilding Research Centre of Japan		62
NETHERLANDS		
Delft Shipbuilding Laboratory		63
Netherlands Ship Model Basin		64
SWEDEN		
Aeronautical Research Institute		65
Statens Skeppsprovvningsanstalt		66
UNITED KINGDOM		
Aeronautical Research Council, Secretary		67
C.A.A.R.C., Secretary		68
National Physical Laboratory, Ship Division		69
Admiralty Experiment Works		70
Ship Model Experiment Tank, Superintendent		71
British Library, Science Reference Library		72
Naval Construction Research Establishment, Superintendent		73
British Ship Research Association		74
Science Museum Library		75
Universities and Colleges		
Bristol	Library, Engineering Department	76
Cambridge	Library, Engineering Department	77
Southampton	Library	78
Strathclyde	Library	79
Cranfield Institute of Technology	Library	80
Imperial College	Library	81
Queens University of Belfast	Dr A. W. Chapleo	82

UNITED STATES OF AMERICA

N.A.S.A. Scientific and Technical Information Facility	83
Applied Mechanics Review	84
Navy Department, Naval Ship Research and Development Center	85
Society of Naval Architects and Marine Engineers	86
Esso Research Laboratories, Director	87

Universities and Colleges

California (Berkeley) Department of Naval Architecture	88
Michigan (Ann Arbor) Department of Naval Architecture	89

SPARES**90-99**